iVES OENO One vine & wine

DOI: https://doi.org/10.20870/oeno-one.2026.60.2.9805

OPEN ACCESS

VITICULTURE ORIGINAL RESEARCH ARTICLES

Berry sugar accumulation and softening dynamics in a slow ripening genotype and its response to hormone application

Pietro Previtali[1,*], Oscar Bellon[2], Elizabeth A. Green[1], Kenneth A. Shackel[3], Marianna Fasoli[2], Sara Zenoni[2], Peter Cousins[1], Megan K. Bartlett[4], Nick K. Dokoozlian[1]

[1] GALLO, Winegrowing Research, 600 Yosemite Blvd, Modesto, CA
[2] University of Verona, Department of Biotechnology, Str. le Grazie, Verona, Italy 37134
[3] University of California Davis, Department of Plant Sciences, 1 Shields Ave, Davis, CA 95616
[4] University of California Davis, Department of Viticulture and Enology, 1 Shields Ave, Davis, CA 95616

Article number: 9805

*correspondence:
pietro.previtali@ejgallo.com

Associate editor:
Eric Gomes

Received:
11 December 2025

Accepted:
12 May 2026

Published:
04 June 2026

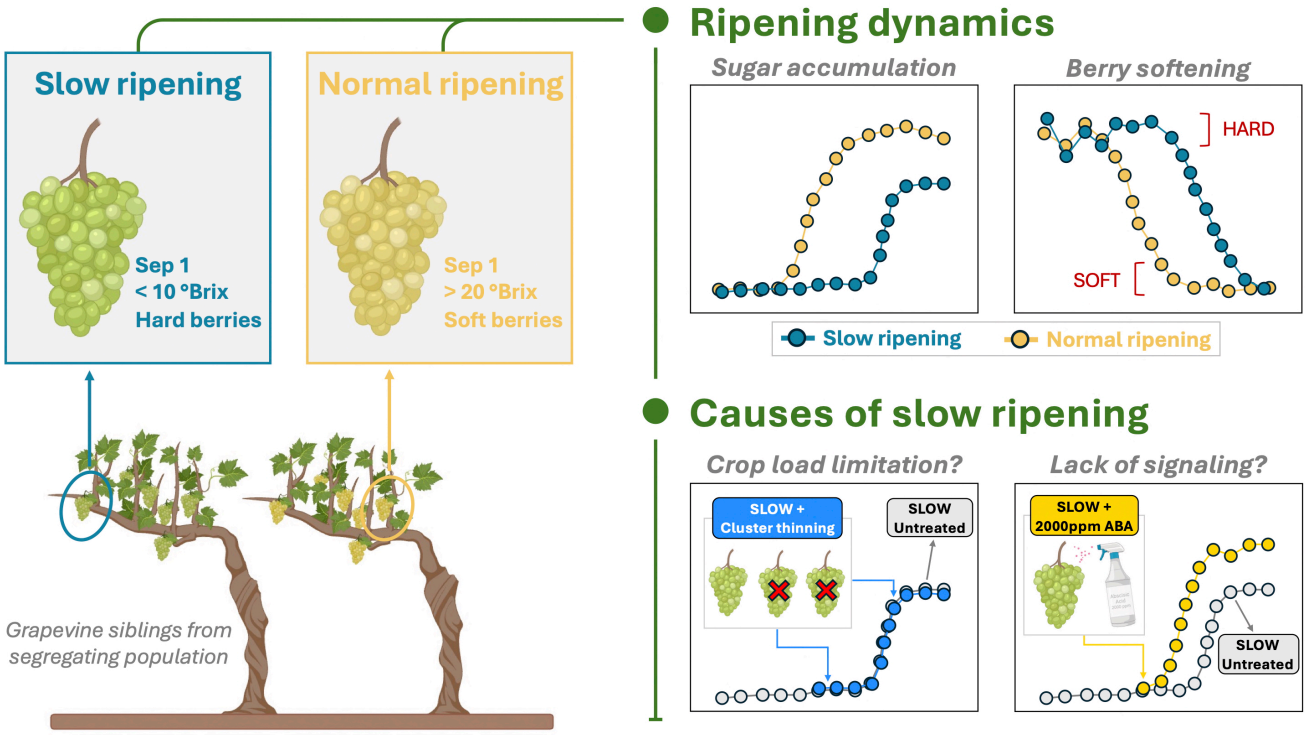
This article is published under the **Creative Commons licence** (CC BY 4.0).

Use of all or part of the content of this article must mention the authors, the year of publication, the title, the name of the journal, the volume, the pages and the DOI in compliance with the information given above.

ABSTRACT

The onset and rate of sugar accumulation in wine grapes are important traits for wine style and quality attainment. As sugar accumulation rates increase due to the consequences of a rapidly changing environment, an uncoupling between the concentration of sugar and other compounds contributing to wine quality is often observed. Management practices can mitigate accelerated sugar accumulation only to a certain extent, while exploration of natural variants with fruit ripening traits of interest represents a more permanent solution. In this study, differences between two full siblings with extreme phenotypic variation in fruit ripening were investigated. Sugar accumulation, berry growth and softening over three years showed an unprecedented ripening delay of over 65 days. Hypothetical causes for the ripening failure were tested through a series of experiments. Leaf physiology was not impaired in the slow-ripening genotype, and severe cluster thinning did not impact ripening time or rate. Abscisic acid treatments promptly triggered sugar accumulation, and treatment efficacy was dependent on the timing and dose applied. These results suggest a potential failure in the signalling process involved in ripening initiation, a first insight towards a fundamental characterisation of mechanisms of slow ripening that could aid selection of improved grape genotypes more suited to future conditions due to climate change.

KEYWORDS: abscisic acid, grape development, hormone application, slow ripening, berry softening, sugar accumulation, water stress



GRAPHICAL ABSTRACT. The graphical abstract was created using Biorender.com.

Abbreviations: ABA, abscisic acid; ACC, 1-aminocyclopropane-1-carboxylic acid; DOY, day of the year; GDD, growing degree days; NR, normal ripening; PEG, polyethylene glycol; SR, slow ripening; SUC, sucrose; TSS, total soluble solids; Ver50, timing of 50 % veraison; WS, water stress.

INTRODUCTION

Viticulture worldwide is threatened by altered patterns in environmental conditions, forcing grapevines to adapt to unprecedented temperatures, rainfall, and CO_2 concentrations (Fraga *et al.*, 2012; Jones & Webb, 2010; van Leeuwen *et al.*, 2024). Grapevine growth and development are highly modulated by environmental conditions, and as such are expected to see repercussions from a changing climate at multiple levels of grape production (van Leeuwen & Darriet, 2016; Mira de Orduña, 2010). Warmer and drier conditions shift grapevine phenology, advancing phenological stages and shortening phenological intervals (Faralli *et al.*, 2024; Fraga *et al.*, 2016; Jones & Davis, 2000; Webb *et al.*, 2007). The ripening process is not exempt from environmental changes, which more often lead to earlier grape maturity (Rogiers *et al.*, 2022; Webb *et al.*, 2011; Webb *et al.*, 2012).

Sugar accumulation in grape berries begins at veraison, at the end of the lag phase and concurrently to the second phase of berry double sigmoidal growth (Coombe, 1992). The physiological processes marking the onset of ripening have been characterised in grapes (Castellarin *et al.*, 2016) and involve a tightly regulated cascade of events, starting with berry softening and abscisic acid (ABA) signalling. This is followed by rapid sugar accumulation and potentially colour development in a second stage. At the transcriptional level, the transition from green to ripening stage is regulated by waves of genes responsible for the activation of ripening-related processes (Fasoli *et al.*, 2018). Early ripeness is seemingly driven by advancing the onset of ripening rather than accelerated ripening rates, the latter being less subject to environmental modulation (Cameron *et al.*, 2021; Sadras & Petrie, 2011). Notably, auxin application delayed and cluster thinning advanced the onset of sugar accumulation, while sugar accumulation rates remained similar to untreated vines (Böttcher *et al.*, 2011; Previtali *et al.*, 2021). One implication of advanced ripening is vintage compression with overlapping harvests across grape varieties or regions, which can result in challenging winery logistics (Jarvis *et al.*, 2019). Additionally, advanced ripening negatively impacts fruit quality due to the decoupling between sugars and metabolites related to acidity, colour, mouthfeel and aroma that are positively associated with wine quality (Previtali *et al.*, 2021; Rienth *et al.*, 2016; Sadras & Moran, 2012; Sadras *et al.*, 2013; Sweetman *et al.*,2014).

Counteractive measures to early grape maturity have been the subject of thorough investigations in the past decades, with the goal of identifying vineyard practices to delay ripening (Gutiérrez-Gamboa *et al.*, 2021; Novello & de Palma, 2013; Palliotti *et al.*, 2014). Among these techniques, antitranspirant sprays, delayed pruning and late source limitation practices have shown a high degree of success across seasons and regions, alongside reduced cost and ease of implementation

commercially (Previtali *et al.*, 2022). Other useful viticultural practices to adapt vineyards to warmer and drier climates have been described, from canopy sprawling to irrigation, crop load management and shading nets for fruit protection (Gutiérrez-Gamboa *et al.*, 2021). While vineyard practices serve as an effective tool for manipulating fruit ripening rates and maturity time in the short term, there are some technical limitations to their implementation. First, their effectiveness plateaus at about a 3-week delay. Second, applications must be planned carefully to avoid multi-seasonal negative effects on yield or vine storage reserves (Poni *et al.*, 2022). A powerful and more long-term option to reduce the pressure exerted by climate change is to leverage natural genotypic variability for the selection of germplasm displaying slower or delayed ripening. Historically, grape varieties and clones have been classified according to their time of commercial maturity, which is typically classified as early-, mid- and late-season ripening. This terminology does not specifically refer to the ripening process (*i.e.* from veraison to a given sugar ripeness), but more generally to the time of harvest or heat summation required for fruit to ripen (Jones, 2010). As pointed out in previous studies, this approach contains bias as it often reflects developmental differences across the entire phenological cycle and not just related to the onset and rate of fruit ripening. Duchêne *et al.* (2012) found that genotypic variability in sugar ripeness was reduced when expressing sugars using thermal scales from veraison to a certain level of heat accumulation. The physiological shift from active sugar accumulation to passive sugar concentration should also be considered, as the sugar concentration at maximum berry growth and the rate of berry weight loss thereafter have been shown to be under a certain degree of genotypic regulation (Deloire, 2011; Shahood *et al.*, 2020; Tilbrook & Tyerman, 2008). Natural variation is the primary driver for crop improvement through traditional breeding programs, and screening of newly developed or pre-existing germplasm has been useful to identify selections better suited to climate change. Frioni *et al.* (2021) and Frioni *et al.* (2023) screened sugars and organic acid levels at harvest in minor autochthonous and newly bred disease-resistant varieties to identify candidates with optimal sugar-to-acidity ratios, better suited for climate change. To date, little focus has been given to the study of genotypic variation in sugar accumulation traits, namely the timing of veraison and the rate of sugar accumulation following veraison. Although the ripening rate does not seem to be modulated by environmental factors, it has been reported to vary on a genotypic basis (Cameron *et al.*, 2021; Stanfield *et al.*, 2024). Significant progress in the -omics sciences applied to grapevine has allowed functional characterisation of genes and regulatory networks governing berry development transitions (Fasoli *et al.*, 2018; Zenoni *et al.*, 2010). However, genes directly controlling the onset and rate of sugar accumulation remain poorly understood (Duchêne *et al.*, 2012). Only recently, natural variation in the so-called speed of ripening trait (*i.e.*, rate of sugar accumulation) has been studied in a segregating population (Falginella *et al.*, 2025). Ripening speed was introgressed in *Vitis vinifera* via hybridisation with *Vitis riparia* and a locus controlling ripening speed was identified. The presence of the RIPENING SPEED locus was associated with a decline in TSS accumulation per day right after veraison, providing a targeted effect on the rate of sugar accumulation without affecting the onset of ripening.

In this study, we characterised physiological differences in the ripening dynamics of two full siblings displaying extreme differences in ripening patterns. A three-year characterisation of sugar accumulation, berry growth and berry softening was performed under field conditions to describe differences in the onset and rate of ripening as well as trait stability over time. In addition, we measured physiological parameters and tested experimental treatments to investigate possible causes for the ripening failure. First, we measured photosynthesis rates to verify potential limitations to carbon assimilation. Second, crop load manipulation was employed to test the possible involvement of limiting source-sink relations in largely delayed fruit ripening. Finally, softening agents, including polyethylene glycol (PEG) and sucrose (SUC), were compared with plant growth regulators [abscisic acid (ABA) and 1-aminocyclopropane-1-carboxylic acid (ACC)] to test whether impeded ripening could be attributed to failing solute accumulation or a lack of hormone signals at the onset of ripening.

MATERIALS AND METHODS

1. Plant material and growing conditions

Plant material evaluated in this study was obtained by cross-breeding in the Breeding and Genetics program at E. & J. Gallo Winery in California. A cross-breeding population was created in 2013 between two white-fruited varieties, from which two proprietary seedlings were selected based on phenotypic observations indicating extreme differences in ripening patterns. One seedling was able to fully ripen (> 20 °Brix) before September 1, called normal ripening (NR), which is considered standard for white-fruited varieties in the area. The other seedling, renamed slow ripening (SR), displayed characteristics commonly associated with pre-veraison fruit on September 1, namely green hard berries. Plots of ten vines for each genotype obtained by vegetative propagation were used for a series of experiments described below. In addition, ten vines of cv. Muscat of Alexandria grown at the same site were added as a reference variety commercially grown in the area. NR and SR own-rooted vines were planted in 2016 near Madera (CA) in homogeneous soil conditions. The soil is a Grangeville series (U.S. Geological Survey, 2024), a fine sandy loam with a high presence of sand (40–60 %) and moderate drainage capacity. Vine distance was 2.1 m and row distance 3 m, and vines were grown as a high-wire bilateral cordon at the height of 1.5 m with a sprawling canopy. All management practices were standardised across the two selections and Muscat of Alexandria, with pruning at 2-bud spurs, no canopy manipulation and full irrigation near 100 % crop evapotranspiration (ETc) monitored using Watermark 200SS soil moisture sensors (Irrometer Company Inc., Riverside, CA). Weather data across the four years of

study were sourced from a local weather station (~1 km from the vine plots). Hourly air temperature, daily rainfall and reference evapotranspiration were recorded. Growing degree days (GDDs) were calculated from April to October using a base temperature of 10 °C and no upper threshold.

2. Characterisation of ripening dynamics

Replicated (n = 3) berry samples were collected from one vine per genotype over 4 years (2022–2025) to characterise sugar accumulation and berry growth kinetics of NR, SR and Muscat of Alexandria. Preliminary data showed that sampling from a single vine captured the same or more variability than across vines (Figure S1A–B). Each sample consisted of nine berries, collected from three clusters and from the top, middle and bottom positions in each cluster. Samples were collected on a weekly basis, and data collection was intensified when possible, close to veraison. Berry samples were weighed to calculate average berry weight and crushed to measure Total Soluble Solids (TSS) using an ATAGO PAL-1 handheld refractometer (Atago Co. Ltd., Bellevue, WA). Sugar content per berry (mg/berry) was approximated by multiplying average berry weight × TSS × 10.

Berry diameter and firmness were measured *in situ* using the GrapeGrabber instrument following the non-destructive procedure detailed in Castellarin *et al.* (2016). Briefly, the elastic modulus of berries was calculated by relating the force applied and the berry displacement measured during berry compression. Firmness calculation, obtained by fitting the Hertz equation in SAS PROC NLIN (version 8.2; SAS Institute), assumes that berries react to compression like a perfectly elastic sphere (Wada *et al.*, 2009). Berry firmness and diameter were measured on six berries per genotype at the same cadence of berry sampling from 2022 to 2024.

3. Experiment 1: Evaluation of differences in leaf physiology and water status

In 2022, vine measurements of leaf water status and gas exchange were taken on Jul 7 (day of the year, DOY 187), Jul 14 (DOY 194), Jul 21 (DOY 201) and Aug 13 (DOY 224). Measurements were taken around solar noon, between 12:30 and 1:30 pm. Leaf water potential (ψ_L) was measured using a 610 PMS pressure chamber (PMS Instruments Co., Albany, OR) on four mature, fully exposed leaves per genotype. On the first three dates, stomatal conductance (gs) was measured on the same leaves using a LI-600 portable porometer (LI-COR Biosciences Inc., Lincoln, NE). On the fourth date, gas exchange parameters (A, net assimilation; gs, stomatal conductance; E, leaf transpiration) were evaluated using a LI-6800 portable photosynthesis system (LI-COR Biosciences Inc., Lincoln, NE), setting reference CO_2 and H_2O conditions to reflect ambient values.

4. Experiment 2: Response to treatments to initiate ripening

Experimental treatments were applied to the SR genotype from 2022 to 2025. The list of treatments applied by year is shown in Figure 1. In 2022, treatments were applied to SR fruit when NR fruit was already ripening to attempt to induce the ripening process. The treatments were named as follows: abscisic acid (ABA), sucrose (SUC), polyethylene glycol (PEG), 1-aminocyclopropane-1-carboxylic acid (ACC) and surfactant (TWEEN). S-abscisic acid (ProTone®, Valent Biosciences, Libertyville, IL) was applied at 400 mg/L (ABA400) and 2000 mg/L (ABA2000) on Aug 4 and Aug 13, respectively. The ABA2000 treatment attempted to increase the effect size observed in preliminary work on ABA400. Sucrose (Sigma-Aldrich Inc., St. Louis, MO) and polyethylene glycol (Sigma-Aldrich Inc., St. Louis, MO) were applied at concentrations of 220 g/L and 380 g/L on

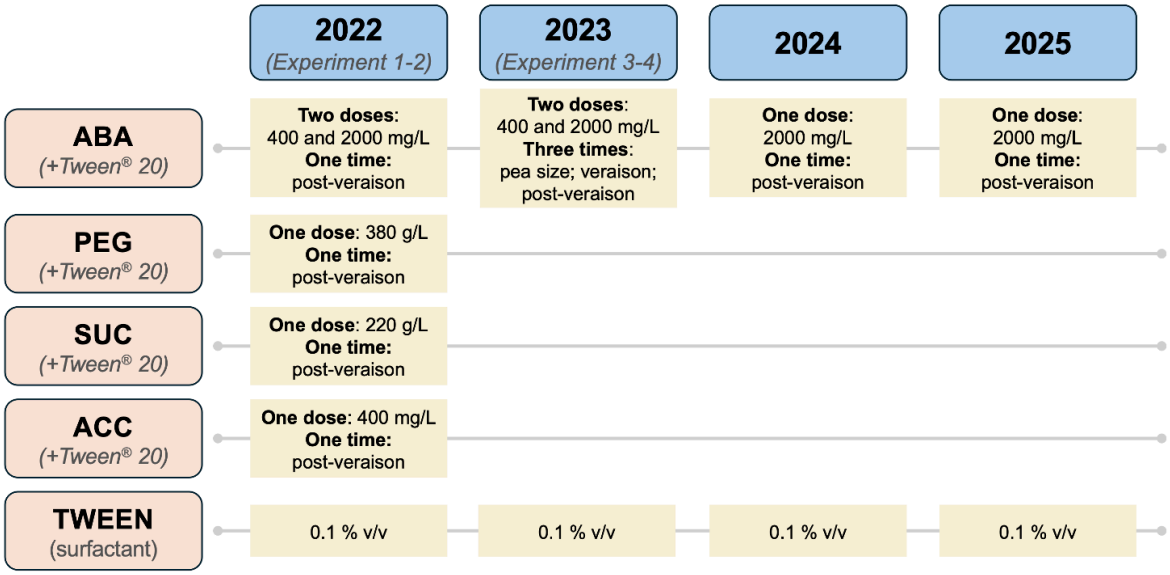


FIGURE 1. Outline of treatments applied to the slow-ripening genotype each year of the study (2022–2025). Abbreviations: ABA, S-abscisic acid; ACC, 1-aminocyclopropane-1-carboxylic acid; PEG, polyethylene glycol; SUC, sucrose.

Aug 4. These doses were calculated based on berry solute concentrations measured on Aug 2, transformed into solute potential and converted into concentrations needed to reduce osmotic potential by 0.5 MPa, to simulate the onset of sugar accumulation. 1-Aminocyclopropane-1-carboxylic acid (Accede®, Valent Biosciences, Libertyville, IL) was applied at 400 mg/L. Tween® 20 (Caisson Labs, Smithfield, UT) was added to all treatments at 0.1 % *v/v* as surfactant and applied as a standalone to account for the effect of spraying. For each treatment, twenty clusters were sprayed to runoff with a handheld sprayer early in the morning. Another twenty clusters were marked at the same time as untreated control.

Treatment effects on berry softening, growth and sugar accumulation were assessed following protocols reported in the previous section. For this experiment, all berries were rinsed with de-ionised water, then gently dried prior to crushing for TSS measurement to avoid interference of product residues on the berry surface.

5. Experiment 3: Response to crop load manipulation

In 2023, crop load was manipulated in one vine of the SR set. Cluster thinning (CT50) was performed on July 24 (DOY 204), leaving one cluster per shoot. Measurements were collected from twenty clusters randomly tagged following the thinning procedure. A second, more severe thinning was applied to the same vine, removing all clusters except for the twenty tagged clusters on Sep 9 (DOY 248). The number and weight of removed clusters were recorded at each pass.

6. Experiment 4: Effect of treatment timing on ripening initiation

In 2023, a factorial study on the effect of the timing and dose of ABA on the SR genotype was conducted. Two doses were tested based on the outcome of Experiment 2: 400 mg/L (ABA400) and 2000 mg/L (ABA2000). Treatment application was repeated at three stages of development of the NR genotype: pea size (PS, DOY 174), veraison (Ver, DOY 208) and post-veraison (Post-V, DOY 235). Protocols for cluster selection, spraying and measurements were the same as in Experiment 2.

7. Experiment 5: Response to water stress

In 2025, responses of SR clusters to exogenous ABA application were compared to those of severe water stress. Based on previous experiments, ABA was applied at 2000 mg/L (ABA2000) post-veraison (DOY 241) and compared to untreated clusters on a separate vine (CONTROL). On the same day of ABA application, dry down of three SR vines was initiated by stopping drip irrigation. Vines were equally irrigated prior to the beginning of water stress. The middle vine was used for subsequent measurements on water-stressed clusters (WS), leaving the neighbouring vines as buffers. The CONTROL and ABA2000 vines were drip irrigated to approximately 100 % ETc. Soil moisture in WS and CONTROL vines was monitored using Watermark 200SS soil moisture sensors (Irrometer Company Inc., Riverside, CA), logging data with 900M Watermark monitors every 30 minutes. Vine response was evaluated using a LI-600 portable porometer (LI-COR Biosciences Inc., Lincoln, NE), measuring three leaves per treatment at solar noon one week after treatment initiation. Stem water potential (ψ_S) was measured on an additional three leaves after conditioning in aluminium bags for a minimum of 30 minutes. Protocols for cluster selection, spraying and fruit sampling were the same as in Experiment 2.

8. Statistical analysis

Data analysis was performed using R (R Core Team, 2012) version 4.3.3 in RStudio (RStudio Inc., Boston, MA). Genotype differences in vine water status and gas exchange were analysed using one-way ANOVA. Significant factors for temporal changes in TSS, berry weight and elasticity were analysed using linear mixed models with the *lmerTest* package (Kuznetsova *et al.*, 2017), selecting genotype and sampling date as fixed effects and replicate and vine as a random effect. Vine number was added as a random effect to account for the sampling procedure explained above (an example of the structural variability of random factors is provided in Figure S1C). In case of significant factors in ANOVA or linear mixed models, means were compared using Tukey's adjusted post-hoc test with an error $\alpha = 0.05$. Mean separation was obtained using the *emmeans* package (Lenth, 2020). TSS and softening curves were modelled using the package *drc* (Ritz *et al.*, 2015).

TSS accumulation curves were fitted using the following equation, which describes a five-parameter logistic regression (Equation 1):

$$y\,(TSS, or\ \frac{mg}{berry}) = y_{max} + \frac{y_{min} - y_{max}}{\left(1+\left(\frac{x}{x_0}\right)^{Slope}\right)^{\varphi}} \quad \text{(Equation 1)}$$

where y represents the response variable (TSS), x represents the explanatory variable (time in days or thermal time as GDDs), y_{min} and y_{max} represent the lower and upper asymptote, respectively, x_0 represents the time at the inflexion point, Slope represents the steepness of the transition between asymptotes and φ represents the asymmetry coefficient. Model fits were evaluated using performance indicators: Akaike Information Criterion (AIC), Residual Sum of Squares (RSS) and the coefficient of determination (R^2). Model significance was tested using the log-likelihood ratio test (LRT), which tests the significance of the full model compared to a null model. TSS accumulation rates were calculated as maximum slopes of the sigmoid curves. Additionally, linear regressions between berry TSS and Julian days or thermal time were calculated, only considering samples from veraison to maximum berry weight that resembled a linear trend.

Firmness data were modelled using inverse four-parameter logistic curves, using the following equation (Equation 2):

$$y\,(Firmness, MPa) = y_{max} + \frac{y_{min} - y_{max}}{1+\left(\frac{x}{x_0}\right)^{-Slope}} \quad \text{(Equation 2)}$$

where the asymptotes and inflexion point are the same as reported for TSS curves, the slope is negative, and there is no asymmetry coefficient φ. Based on softening curves, the inflection point x_0 was assumed to be the DOY at which 50 % veraison was achieved (Ver50).

All visualisations were produced using the package *ggplot2* (Wickham, 2016).

RESULTS

1. Seasonal weather patterns

Differences in seasonal temperature and heat accumulation are shown in Figure 2. According to GDD summation curves (Figure 2A), 2022 and 2024 were hotter seasons (2897 and 2929 total GDD accumulated, respectively) compared to 2023 and 2025 (2646 and 2742 GDD in total). Temporal distribution of heat spikes was season-dependent (Figure 2B). In 2022, there was a sustained period of heat in the middle of the season, starting in July and leading up to September. In 2023 and 2024, temperature peaked in July, with a more pronounced spike in 2024, and started dropping thereafter.

2. Berry ripening dynamics: berry growth, softening and sugar accumulation

Dynamics of berry growth, TSS accumulation and berry softening for the genotypes over the three years of study are shown in Figure 3. The cadence of TSS measurements in 2022 was not enough to fully determine the initiation of ripening in NR (Figure 3A). In 2023 and 2024, data collection was started earlier, capturing ripening earlier and at a higher resolution across the three genotypes (Figure 3B–C). Based on these measurements, ripening was most advanced in the NR genotype, followed by Muscat of Alexandria. SR had a consistent delay in the onset of sugar accumulation until after the NR individual had reached its plateau at about 20 °Brix. Using 8–9 °Brix as a proxy for veraison, TSS stalled below this threshold for a long period in SR all three years. TSS curves of Muscat of Alexandria were intermediate between SR and NR in both 2022 and 2023 but became much closer to NR than SR in 2024. The results of models fitted to TSS data are shown in Table 1. Compared to three- and four-parameter models, five-parameter sigmoidal curves resulted in improved fits (Figure S2) and model performance metrics (Table S1) for TSS observations. Five-parameter models well described relationships between TSS data and DOY or GDD, with $R^2 \geq 0.965$ across the board. Lower and upper asymptote estimates were the same for both models. There was a consistent difference in the upper asymptote by genotype, representing the maximum TSS levels reached at the end of the ripening curve, which never surpassed the threshold of 18 °Brix across the three years in SR fruit while being well above 20 °Brix in NR. For the model of TSS by chronological time (DOY), all parameters were influenced by the interaction between genotype and year ($p = 0.019$ or lower) except for the curve slope and asymmetry coefficient φ, for which the genotype was the only significant factor ($p < 0.001$). The inflection point x_0, representing the midpoint of the active

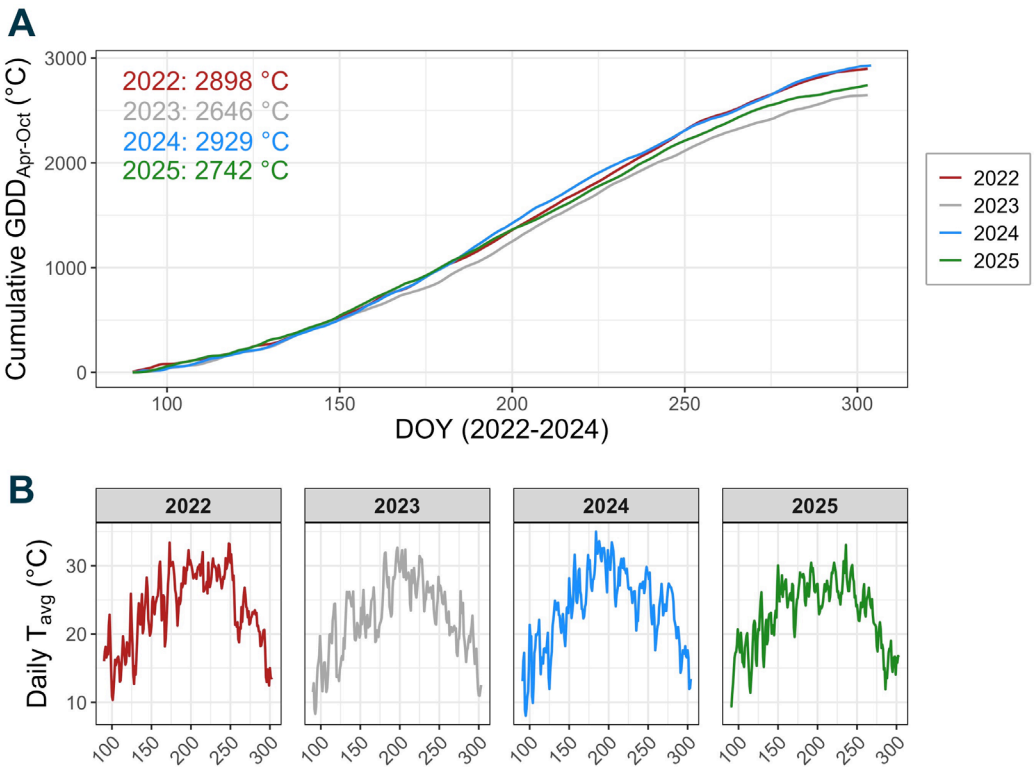


FIGURE 2. Growing season weather conditions for the four years of study. A) Curves of growing degree days (GDD) accumulation and B) daily average temperature (Tavg) by year. Colours differentiate between years: 2022 (red), 2023 (grey), 2024 (blue) and 2025 (green). Abbreviations: DOY, day of the year.

sugar accumulation phase, was largely and consistently delayed in SR compared to NR (76 days on average) and Muscat of Alexandria (73 days on average). Fruit ripening rate, expressed as the TSS/day ratio at the inflexion point, was impacted by the genotype *x* year interaction ($p = 0.007$), and it was higher in NR compared to SR and Muscat of Alexandria (both $p \leq 0.001$) and unchanged between the latter two genotypes ($p = 0.476$) in 2023 and 2025. In 2024, differences in TSS/day were not significant between the three genotypes (all $p \geq 0.134$). In the model of TSS by GDD, there was only a significant effect of the genotype on curve parameters, namely x_0, slope and the GDD-based ripening rate (all $p \leq 0.002$). The rate of TSS increase per 100 GDD accumulated was lowest in Muscat of Alexandria (1.21 °Brix/100 GDD) and significantly increased in both NR (2.53 °Brix/100 GDD, $p = 0.002$) and SR (2.24 °Brix/100 GDD, $p = 0.015$). The GDD-based ripening rate was unchanged between NR and SR fruit ($p = 0.657$). Statistical outputs of five-parameter sigmoid models applied to sugar content estimates per berry are shown in Table S2. Sugar content models displayed slightly lower R^2 values compared to TSS ones, but the overall performance of the fits was high (≥ 0.914 for the DOY model, except for Muscat of Alexandria in 2025; ≥ 0.921 for GDD models). Similar to the TSS models, parameters extracted for sugar content estimates modelled against DOY were affected by the interaction of genotype and year, while expressing sugar content by GDD resulted in significant effects only for the genotype factor ($p < 0.001$ for x_0, slope and GDD-based ripening rate). According to the GDD-based model, Muscat of Alexandria had the highest sugar loading rate (52.6 mg/100 GDD), compared to which NR and SR rates were significantly reduced to 29.8 ($p = 0.021$) and 27.2 mg/100 GDD ($p = 0.013$), respectively. NR and SR sugar loading rates were not significantly different ($p = 0.940$). Linear regressions in the range from Ver50 to maximum sugar content expressed by the DOY and GDD scales were explored for TSS (Figure S3) and sugar content estimates (Figure S4). Corrections to the GDD scale were also applied to test the effect of capping GDD calculations at 30 °C; however, this did not affect the results. Results of linear models were in line with the outputs of the sigmoid curves.

Sampling was started late in 2022, and full curves of berry growth were not obtained (Figure 3D). In 2023 and 2024, berry growth (Figure 3E–F) followed a double sigmoid curve, and the shape of this curve was impacted by both genotype and year. Berries of Muscat of Alexandria quickly became significantly larger than NR and SR irrespective of the year. There were evident differences between 2023 and 2024, with higher maximum berry weight and higher levels of late-season dehydration occurring in 2023. The effect of the year on TSS and berry growth dynamics was more marked in NR and Muscat of Alexandria compared to SR.

Changes in firmness values by genotype from 2022 to 2024 are depicted in Figure 3G–I. In 2022, measurements were started when berries of the NR genotype and Muscat of Alexandria were already soft (firmness < 1 MPa). In SR, there was an early drop in firmness in 2022 (Figure 3G), then typical pre-veraison firmness was recovered (> 4 MPa). The full transition from hard (> 4 MPa) to completely soft (< 1 MPa) started around DOY 240. Increased frequency of sampling in 2023 (Figure 3H) and 2024 (Figure 3I) allowed us to fully describe the timing and kinetics of softening for all genotypes. In both years, there were fluctuations in firmness earlier in the season preceding the final drop in firmness to fully soft berries. Inverse sigmoid fits are shown in Figure S5 and softening parameters extrapolated from the fits are reported in Table 2. Ver50 occurred on the same DOY 187 in NR in 2023 and 2024 and was delayed by 68 and 66 days in SR, respectively. For Muscat of Alexandria, Ver50 occurred 17 and 8 days after NR in 2023 and 2024, respectively. The curve slope, representing how quickly the berry population completed softening, was highest in Muscat of Alexandria in both years when full curves were obtained. In 2023, the slope was lower in NR compared to SR, while the opposite trend was observed in 2024.

3. Experiment 1: Exploration of genotype-specific vine physiology traits

Midday stomatal conductance (gs) and leaf water potential (Ψ_L) measured for the three genotypes at three dates are shown in Figure 4A–B. At all July dates (DOY 187, 194 and 201), there were no differences in gs values between NR and SR, while gs was consistently lower in Muscat of Alexandria. In turn, water status was higher in Muscat of Alexandria (Ψ_L: –1.02 MPa) compared to both NR (–1.40 MPa) and SR (–1.31 MPa) at the first sampling date. At subsequent dates, Ψ_L values declined in both Muscat of Alexandria and NR, while remaining relatively constant in SR. As a result, NR vines were significantly more stressed than SR and Muscat of Alexandria at DOY 194 and 201. According to gas exchange measurements taken on DOY 224 (Figure 4C), differences in A_{net} between SR and NR were barely insignificant ($p = 0.055$), while both gs and E rates were increased in SR (gs: $p = 0.037$; E: $p = 0.039$). Muscat of Alexandria vines displayed the lowest levels of A_{net}, gs and E across the genotypes investigated. In 2024 (DOY 227), the separation between SR and NR was more evident: the highest A_{net}, gs and E values were recorded in SR, with a significant decline in both NR and Muscat of Alexandria.

4. Experiment 2: Response to hormone treatments

Softening and TSS accumulation curves for treated SR clusters in comparison to untreated ones are shown in Figure 5. According to TSS accumulation curves, the only treatment that was able to advance the onset of sugar accumulation in SR was ABA2000 (Figure 5A). The first significant increase in TSS for ABA2000 compared to the control happened on DOY 236. The TSS value at this date (9.2 °Brix) indicated the rapid phase of sugar accumulation had started. The onset of ripening did not happen until around DOY 262 (8.3 °Brix) for untreated clusters. This represents a 26-day delay in the onset of sugar accumulation. After DOY 257, the rate of TSS accumulation in ABA2000 became much slower, with differences from the control disappearing

TABLE 1. Statistical parameters of Total Soluble Solids (TSS) accumulation models fitted on three years of data (2023–2025).

	TSS by DOY							TSS by GDD			
	Lower	Upper	x_0 (DOY)	Slope	Rate (TSS/day)	φ	R^2	x_0 (GDD)	Slope	Rate (TSS/100 GDDs)	φ	R^2
2023												
Normal Ripening	4.22 a[a]	30.4 a	202 b	0.081 b	0.560 a	0.97 a	0.976	1303 b	0.004 b	2.98 a	0.98 a	0.989
Slow Ripening	4.79 a	17.8 b	275 a	0.141 a	0.294 b	0.64 a	0.981	2466 a	0.003 b	2.62 a	0.64 b	0.980
Muscat of Alexandria	4.54 a	20.7 b	216 b	0.057 b	0.231 b	1.35 a	0.982	1315 b	0.160 a	0.96 b	7.06 a	0.980
2024												
Normal Ripening	5.35 b	24.3 a	202 b	0.088 b	0.404 a	1.17 a	0.985	1431 b	0.005 a	2.20 a	1.08 a	0.992
Slow Ripening	5.97 a	17.7 b	271 a	0.123 a	0.295 a	0.26 b	0.965	2647 a	0.010 a	1.98 a	0.44 a	0.987
Muscat of Alexandria	4.53 c	24.6 a	203 b	0.067 b	0.357 a	1.55 a	0.989	1385 b	0.004 a	1.63 a	1.30 a	0.984
2025												
Normal Ripening	5.90 a	25.2 a	197 b	0.105 b	0.522 a	1.22 b	0.995	1217 b	0.007 b	2.62 a	1.09 ab	0.996
Slow Ripening	5.45 a	16.0 b	285 a	0.110 a	0.198 b	0.26 c	0.982	2676 a	0.018 a	1.89 ab	0.36 b	0.990
Muscat of Alexandria	4.78 b	25.1 a	192 b	0.065 b	0.193 b	2.40 a	0.991	1126 b	0.004 b	1.03 b	5.23 a	0.977
Statistics[b]												
Genotype	< 0.001 (***)	< 0.001 (***)	< 0.001 (***)	< 0.001 (***)	< 0.001 (***)	< 0.001 (***)		< 0.001 (***)	< 0.001 (***)	0.002 (**)	0.002 (**)	
Year	< 0.001 (***)	0.017 (*)	0.207	0.996	0.172	0.238		0.354	0.369	0.572	0.203	
Genotype x Year	0.010 (*)	< 0.001 (***)	0.019 (*)	0.491	0.007 (**)	0.086		0.621	0.71	0.288	0.196	

Notes: sigmoid curves from which model parameters were extracted are reported in Figure S2. Except for R^2 values, estimates by genotype and year are presented as means (n = 3). Abbreviations: DOY, day of the year; GDD, growing degree days; Lower, lower asymptote; TSS, total soluble solids; Upper, upper asymptote; x_0, inflexion point; **φ**, asymmetry coefficient.

[a] Different letters denote significant differences according to ANOVA and Tukey's adjusted post-hoc test ($p < 0.05$).

[b] P(F) values according to ANOVA.

TABLE 2. Model parameters extrapolated from softening curves for each genotype and year.

	Softening		
	Slope	Ver50 (DOY)	R^2
2022			
Normal ripening	/	/	0.298
Slow ripening	45.21	265	0.702
Muscat of Alexandria	/	/	0.185
2023			
Normal ripening	22.97	187	0.858
Slow ripening	39.09	255	0.722
Muscat of Alexandria	101.90	204	0.852
2024			
Normal ripening	52.46	187	0.933
Slow ripening	19.57	253	0.680
Muscat of Alexandria	92.61	195	0.864
2025			
Normal ripening	/	190	/
Slow ripening	/	261	/
Muscat of Alexandria	/	198	/

Notes: firmness data were modelled using a four-parameter log logistic regression curve. Inverse sigmoid curves from which softening parameters were calculated are reported in Figure S5. Softening parameters for 2022 are not available for normal ripening and Muscat of Alexandria due to the late start of fruit sampling. In 2025, firmness was not measured, and veraison dates were approximated based on average TSS levels at Ver50 in previous years. Abbreviations: DOY, day of the year, Ver50, time of 50 % veraison.

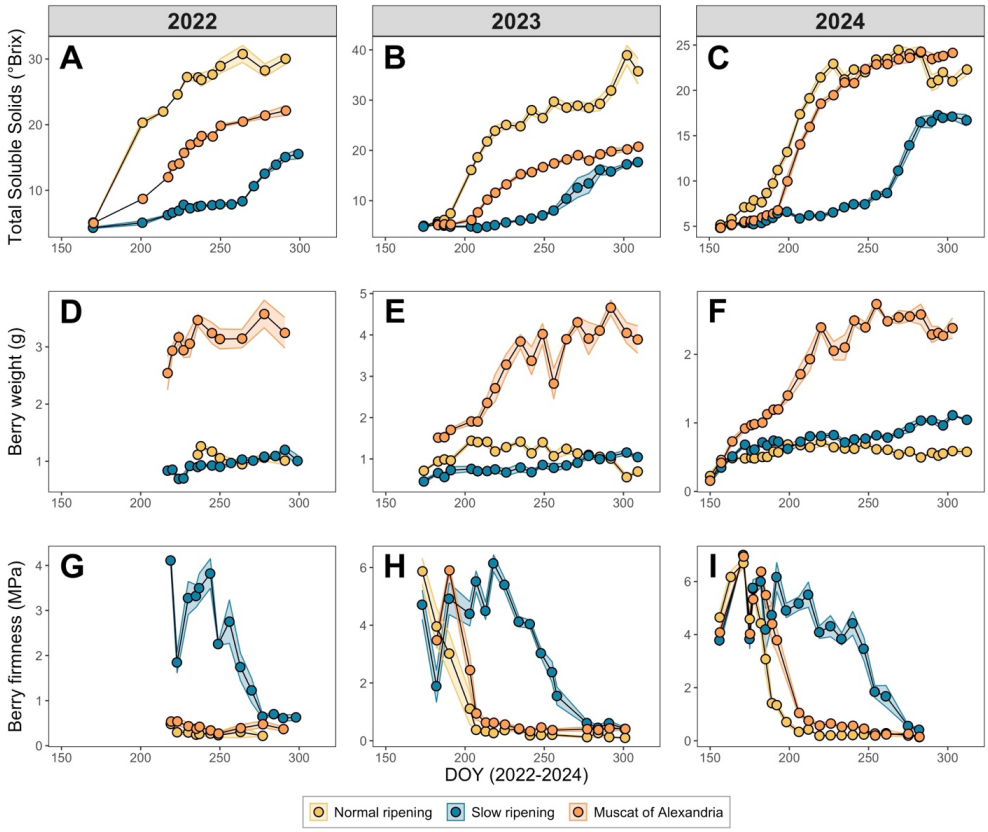


FIGURE 3. Changes in total soluble solids (TSS) (A–C), berry growth (D–F) and berry firmness (G–I) for the genotypes investigated over three years: 2022 (A, D, G), 2023 (B, E, H) and 2024 (C, F, I). Colours differentiate between genotypes: normal ripening (yellow), slow ripening (blue) and Muscat of Alexandria (orange). Points and ribbons represent means and SE values (n = 3 for TSS and berry weight; n = 6 for berry firmness). Statistical comparisons for TSS, berry growth and berry firmness at each date are reported in Table S3 (TSS), Table S4 (berry weight) and Table S5 (firmness), respectively. Abbreviations: DOY, day of the year; TSS, total soluble solids.

from DOY 278. Comparing softening patterns in ABA2000 and untreated clusters (Figure 5B), there was a significant reduction in berry firmness in ABA2000 berries shortly after the treatment on DOY 236 (1.2 MPa), concomitant with the increase in TSS values. Firmness levels in the control remained in the range typically associated with hard preveraison berries (3.3 MPa). TSS and softening curves in ABA2000 were parallel to those drawn for untreated clusters, while the slopes were equal, indicating an effect largely on the onset and not on the rate of ripening. When a lower dose of ABA was applied (ABA400), the advancing effect was not as evident as in ABA2000. TSS values in ABA400 were significantly higher at two dates preceding the onset of ripening in untreated clusters, namely DOY 257 (9.4 *vs* 7.8 °Brix, $p = 0.008$) and 262 (10.1 *vs* 8.3 °Brix, $p = 0.002$). In the case of ACC, there was a transient effect on TSS values around veraison (DOY 262), which were significantly higher (10.2 °Brix) than the control (8.3 °Brix, $p < 0.001$). Softening curves of berries treated with ABA400 and ACC were largely unaffected by the treatment applied, except for a few early dates showing transient differences. PEG application did not affect the onset of ripening, but it led to consistently higher TSS values compared to the control during the ripening stage, starting from DOY 271. When SUC was applied, there were also negligible effects on TSS accumulation and on berry softening. Lastly, the application of Tween did not alter berry firmness patterns but led to small significant increases in berry TSS at the end of the sugar accumulation process, starting from DOY 299.

5. Experiment 3: Response to crop load manipulation

On the first cluster thinning pass (DOY 204), 52 clusters were removed, equalling to 13 kg of fruit. The second thinning exercise executed on DOY 248 exported an additional 45 clusters for an additional 12 kg of fruit removed from the vine. The final vine yield for the two vines was 30.5 kg (98 clusters) for the untreated control and 3.5 kg (10 clusters) in CT50. The effect of this two-step cluster thinning on the kinetics of sugar accumulation and berry firmness is represented in Figure 6. Crop removal did not advance the

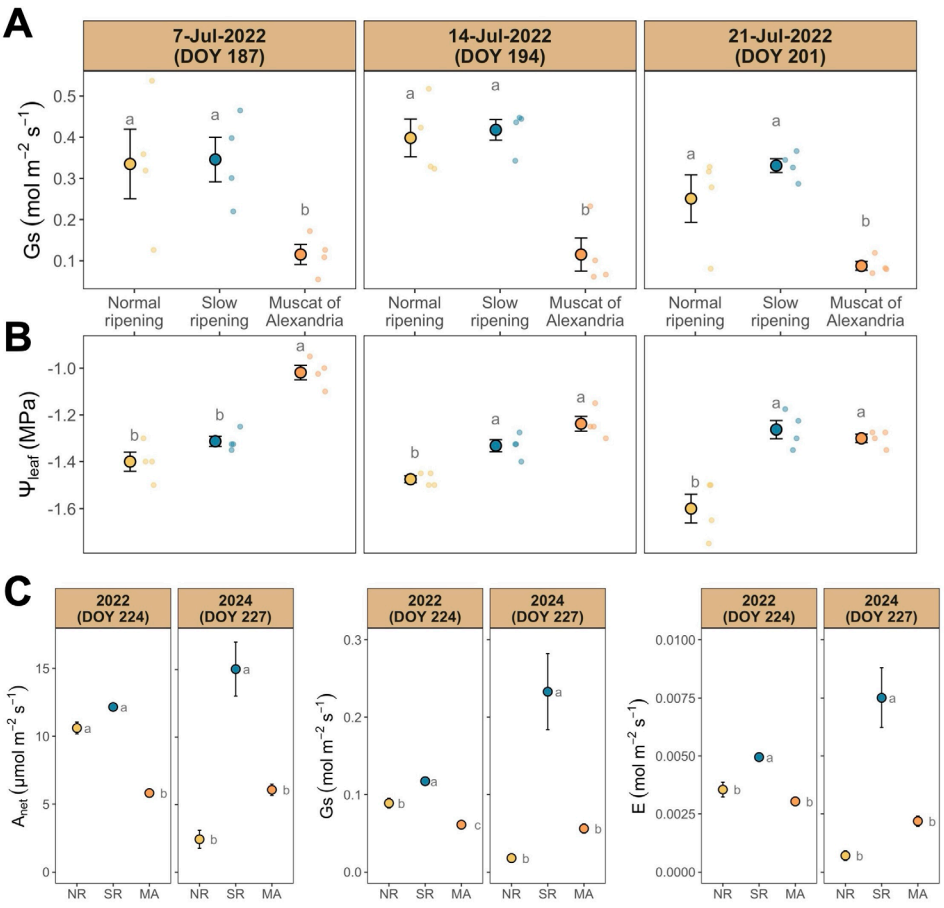


FIGURE 4. Water status and vine physiology differences between the genotypes investigated: A) stomatal conductance (gs); B) leaf water potential (ψ_L) and C) leaf gas exchange parameters (A_{net}, net CO_2 assimilation; gs, stomatal conductance; E, transpiration). Measurements in C were taken on Aug 13 in 2022 (DOY 224) and Aug 15 in 2024 (DOY 227). Data by year are reported side by side for each parameter, using the same scale for comparison. Points and error bars represent means and SE values by genotype (A–B, $n = 4$; C, $n \geq 3$). Smaller points represent raw measurements. Letters denote significant differences according to one-way ANOVA followed by Tukey's adjusted post hoc test ($\alpha \leq 0.05$). Colours discriminate between genotype: normal ripening (NR, yellow); slow ripening (SR, blue) and Muscat of Alexandria (MA, orange).

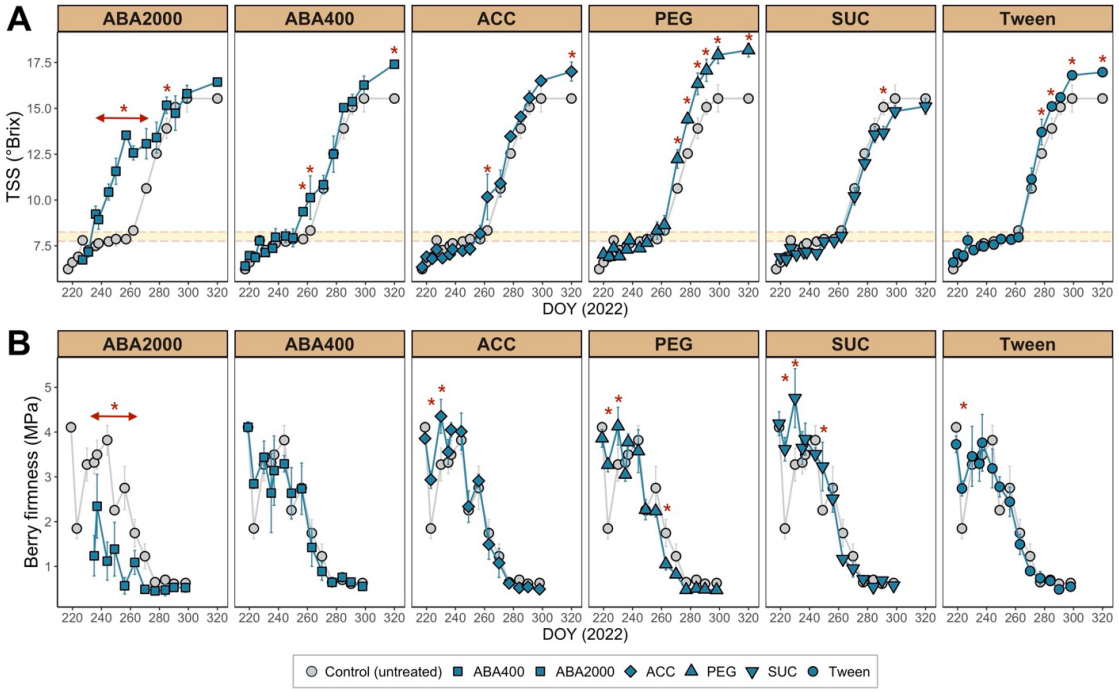


FIGURE 5. Comparison of sugar accumulation (A) and softening curves (B) in treated and untreated clusters of the slow ripening genotype. Each panel represents an experimental treatment: ABA2000 (abscisic acid at 2000 mg/L); ABA400 (abscisic acid at 400 mg/L); ACC (Accede); PEG (polyethylene glycol); SUC (sucrose) and Tween (surfactant). In each panel, colours differentiate between treated (blue) and untreated (grey) clusters. Points and error bars represent means ± SE values (n = 3 for A; n = 6 for B). Asterisks denote significant differences between treated and control means according to Tukey's adjusted post hoc test ($\alpha \leq 0.05$). Estimates and p-values for each contrast are reported in Table S6 (TSS) and Table S7 (Firmness). Yellow rectangles in A represent the TSS interval corresponding to veraison according to the literature (around 8 °Brix). Abbreviations: TSS, total soluble solids; DOY, day of the year.

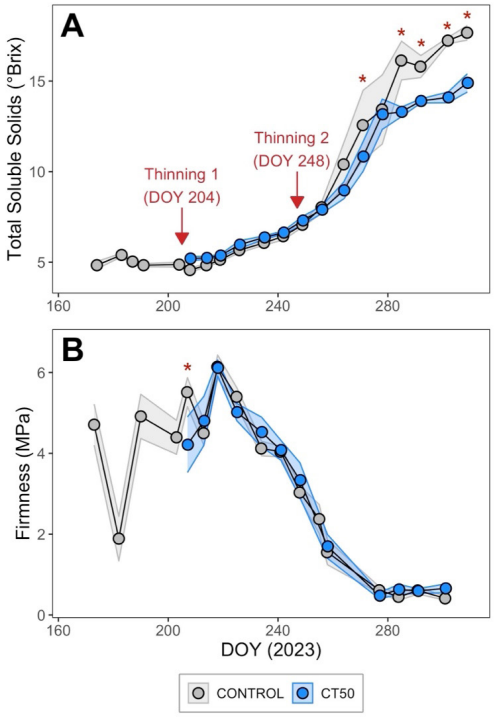


FIGURE 6. Effect of crop load manipulation on sugar accumulation (A) and softening dynamics (B) of the slow ripening genotype. Points and ribbons represent means ± SE (n = 3 for TSS; n = 6 for firmness). Colours differentiate between cluster thinning (CT50, in blue) and untreated (CONTROL, in grey). Red arrows and text indicate the timing of two cluster thinning passes. Asterisks indicate significant differences between treated and control means according to Tukey's adjusted post hoc test ($\alpha \leq 0.05$). Estimates and p-values for each contrast are reported in Table S8 (TSS) and Table S9 (Firmness). Abbreviations: DOY, day of the year.

onset of sugar accumulation nor did it accelerate ripening (Figure 6A). Similarly, except for the very first sampling date, severe cluster thinning did not affect softening curves (Figure 6B). TSS values measured in CT50 berries at the last four sampling dates were significantly lower compared to the control (between 2 and 3 °Brix on average), displaying a lower TSS plateau compared to the control.

6. Experiment 4: Effect of ABA application timing on ripening kinetics

The response of the SR genotype to ABA treatments applied at three different times based on the development of the NR sibling, namely pea-size, veraison and post-veraison, is illustrated in Figure 7. Neither of the applied ABA doses (400 *vs* 2000 mg/L) was able to trigger ripening at the first two timings, namely when the NR genotype was at the pea size (Figure 7A–B) and veraison stages (Figure 7D–E). When ABA400 was applied at pea size (Figure 7A), there were transient significant differences compared to the control at DOY 271 (–1.9 °Brix, p = 0.022) and 285 (–1.8 °Brix, p = 0.027). TSS accumulation curves of ABA2000 and Tween applied at pea size (Figure 7B–C) were comparable and appeared to be delayed compared to the control, as indicated by significantly lower TSS values compared to the control starting from DOY 264. Sugar accumulation curves for the three treatments when applied at the veraison stage of NR completely overlapped with those of untreated clusters (Figure 7D–F). Post-veraison treatments (Figure 7G–I) had the largest effect on sugar accumulation, leading to a significant advancement of ripening. Starting from 256, TSS values were consistently higher in ABA400 compared to the control (2.5 °Brix on average, $p \leq 0.001$), an approximate ripening advancement of 7 to 10 days. The effect of ABA was even more marked with the highest dose applied (ABA2000, Figure 7H), which caused an earlier onset (from DOY 249) and a larger (5.3 °Brix on average, $p < 0.001$) increase in TSS accumulation. Tween application post-veraison did not affect the onset or rate of sugar accumulation but appeared to increase the plateau of TSS accumulation, still to a lower extent compared to ABA2000.

Softening curves measured in ABA treatments and control clusters confirmed TSS results (Figure 7J–K). In ABA400, there was a trend for lower firmness following treatment application; however, no significant differences were found. In contrast, the application of ABA2000 caused a quick significant drop in firmness, indicated by large significant drops in firmness values compared to the control, allowing ABA2000-treated berries to reach full softness earlier.

7. Experiment 5: Effect of water stress on ripening kinetics

Soil water tension patterns for water-stressed and normally irrigated SR vines are shown in Figure 8A. Once watered at DOY 244, water tension in CONTROL vines promptly decreased to close to zero and then gradually increased over the following two weeks. In contrast, soil remained dry under WS vines where irrigation was not applied. When shrivelling symptoms started to appear, irrigation was supplied to WS vines on DOY 252, as observed in the decrease of soil tension values below the irrigation threshold set at 60 cbar. A second dry down was applied from DOY 254 to 265, resulting in a pronounced water tension increase in WS vines compared to the irrigated control. The effect of ceased irrigation on SR vine performance is shown in Figure 8B. At DOY 247, there was a significant decrease (p = 0.0001) in midday Ψ_S in WS vines (–1.43 MPa) compared to the CONTROL (–1.02 MPa). Water status differences between WS and CONTROL vines were maintained one week later ($\Delta\Psi_S$ = 0.3 MPa, p = 0.001) (data not shown). Gs was not significantly different in CONTROL and ABA2000 vines at DOY 247 (p = 0.998); in contrast, WS vines had significantly lower gs values (p = 0.013 or lower). Responses of fruit TSS levels to ABA2000 and WS treatments are presented in Figure 8C. In both treatments, TSS levels were significantly increased at each of the 11 sampling times following treatment application. As for the comparison between ABA2000 and WS fruit, TSS means were unchanged only at the first sampling point after treatment initiation (DOY 248, ΔTSS = 0.87 °Brix, p = 0.459), and TSS were higher in ABA2000 than WS at all following dates (p = 0.017 or lower). Changes in BW and sugar per berry for the three treatments are compared in Figure S7. Sugar content estimates reflected trends observed for TSS values. BW sharply increased in ABA2000-treated clusters compared to CONTROL, but the same effect was not as evident nor always significant for WS. The results of five-parameter logistic regression curves on TSS and sugar content observations by treatment are shown in Table S11, and individual fits per replicate and treatment are shown in Figure S7. SR treatments significantly affected the inflection point x_0 in both TSS and sugar content curves ($p \leq 0.004$). The TSS/day ratio was higher in ABA2000 (0.83 °Brix/day) compared to both CONTROL (0.22 °Brix/day) and WS (0.24 °Brix/day).

DISCUSSION

1. Onset and rate of ripening in the slow ripening genotype

Berry growth, sugar accumulation and berry firmness data were collected at high temporal resolution over four years for the SR and NR genotypes plus a reference variety, Muscat of Alexandria. Temporal changes in these parameters are the cornerstone for the understanding of physiological processes associated with the beginning of ripening, as described in Castellarin *et al*. (2016). When comparing sugar accumulation curves, overall trends were consistent across the four years, with the NR genotype displaying the earliest ripening, SR being the most delayed and Muscat of Alexandria falling in the middle (Figure 3A–C). Softening curves built from berry firmness measurements (Table 2) were used to calculate the timing of 50 % veraison (Ver50, *i.e.*, the inflexion points of the firmness curve). As shown in Figure S6, expressing TSS values as a function of the days post Ver50 resulted in aligned curves for 2023, 2024 and 2025. By comparing Ver50

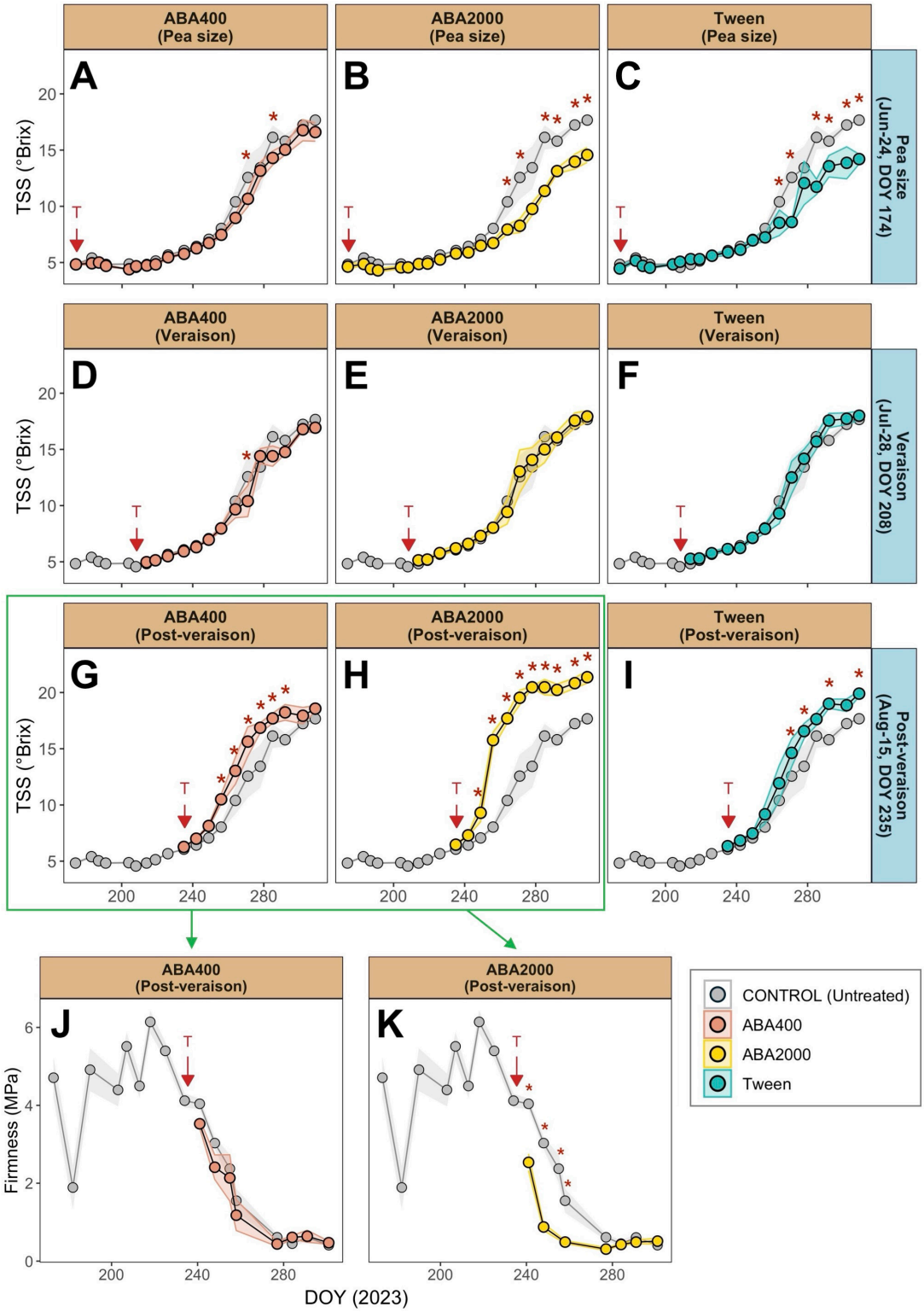


FIGURE 7. Effect of dosage and timing of abscisic acid (ABA) application on kinetics of sugar accumulation (A–I) and softening (J–K) of the slow ripening genotype (SR). ABA was applied at two concentrations: 400 mg/L (ABA400) and 2000 mg/L (ABA2000). Tween represents the application of surfactant only. Treatments were applied at three stages of development of the normal ripening genotype (NR): pea size (A–C), veraison (D–F) and post-veraison (G–I). Softening curves are shown for the two treatments that advanced the onset of sugar accumulation, both applied post-veraison: ABA400 (J) and ABA2000 (K). Points and ribbons represent means ± SE (n = 3 for TSS, n = 6 for firmness). Colours differentiate between treatments: CONTROL (grey), ABA400 (pink), ABA2000 (yellow) and Tween (turquoise). Red arrows and text indicate dates of treatment application. Asterisks denote significant differences between treated and control means according to Tukey's adjusted post hoc test ($\alpha \leq 0.05$). Abbreviations: TSS, total soluble solids; DOY, day of the year.

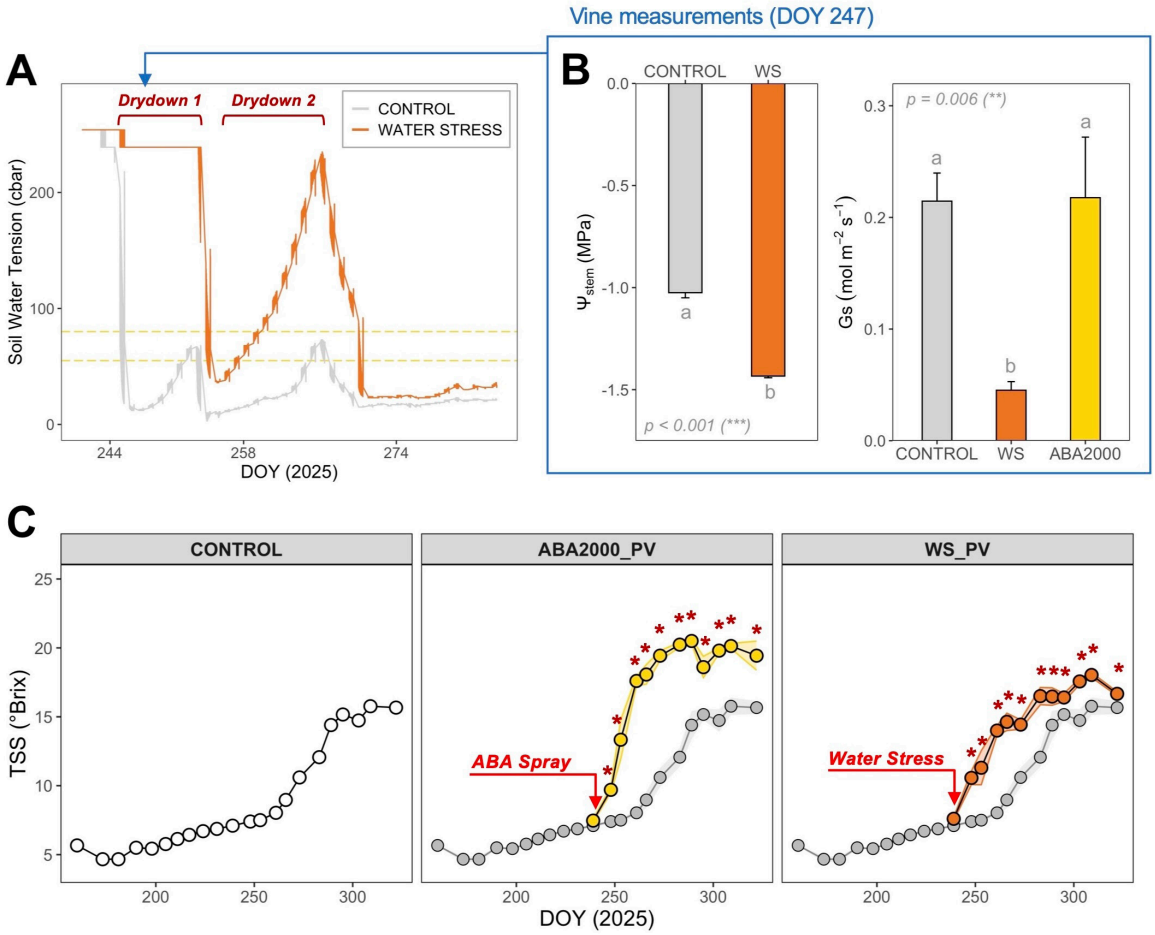


FIGURE 8. Effect of water stress and application of exogenous abscisic acid (ABA) on vine performance and ripening kinetics in the slow ripening genotype. A) Soil water tension measured at 30 cm depth in irrigated (CONTROL) and water-stressed (WS) vines. Yellow dashed lines represent the critical threshold (60–80 cbar) used to schedule irrigation at the site. B) Vine response to ABA and WS treatments in the slow ripening genotype, including stem water potential (Ψ_{Stem}) and stomatal conductance (gs). Bars and error bars indicate means ± SE by treatment (n = 3). Letters denote statistical differences according to ANOVA followed by Tukey's adjusted post hoc test at $\alpha \leq 0.05$. *P*-values indicate statistical significance of ANOVA models for the Treatment factor. C) Total Soluble Solids (TSS, in °Brix) curves by treatment. Points and ribbons represent means ± SE (n = 3). Red arrows and text indicate dates of treatment application. Asterisks denote significant differences between treated and control groups according to Tukey's adjusted post hoc test ($\alpha \leq 0.05$). Statistical comparisons of TSS by treatment at each date are reported in Table S10. Across the board, colours differentiate between treatments: untreated (CONTROL, white/grey), ABA at 2000 mg/L (ABA2000, yellow) and water stress (WS, orange). Abbreviations: TSS, total soluble solids; DOY, day of the year.

across genotypes, differences in ripening initiation were anchored to a fixed physiological parameter, namely, half of the berries softened. This approach overcomes the effect of longer or shorter transitions from pre- to post-veraison stages, driven by the highly asynchronous development of berry populations across genotypes and possibly introducing bias in the interpretation of temporal changes (Shahood *et al.*, 2020; Tavernier *et al.*, 2025). Over the two years when this approximation could be made, Ver50 was delayed 68 and 66 days in SR compared to NR. Firmness data were not collected in 2025, but an approximation of the Ver50 value based on relationships between TSS and firmness in previous years resulted in 71 days of delay, which is consistent with the previous two seasons (Table 2). Extensive research has been dedicated to the identification of strategies to delay ripening, to counteract advanced grape maturity driven by warmer and drier conditions (Gutiérrez-Gamboa *et al.*, 2021; Palliotti *et al.*, 2014; Previtali *et al.*, 2022). At the study location, classified as a hot and dry Mediterranean climate, delaying veraison by over two months signifies that ripening starts at the end rather than the start of summer. Delayed ripening therefore offers benefits in terms of reduced organic acid degradation, slower sugar accumulation and improved colour, phenolic and aroma compounds that are sensitive to high temperature (Mori *et al.*, 2007; Previtali *et al.*, 2021; Sadras & Moran, 2012; Sweetman *et al.*, 2014). It is important to note that the delay observed in the SR genotype is much greater than the effect obtained using vineyard practices to delay ripening, where the maximum delay is about three weeks (Previtali *et al.*, 2022). Additionally, the

effect size of these management practices is variable, and yield declines are sometimes a trade-off for the ripening delay (Poni *et al.*, 2022). Exploring genetic material could not only offer a longer-term solution, but also a potentially more stable solution since slow ripening is de-associated from other effects observed when the delay is achieved by in-season manipulation of grapevines.

One important aspect that needs clarification for a comprehensive understanding of the slow ripening selection evaluated in this study is the relative importance of ripening rate and ripening onset in determining the final delay at harvest. Data mining studies (Cameron *et al.*, 2021) and manipulatory studies (Böttcher *et al.*, 2011; Previtali *et al.*, 2021) provide evidence to support the hypothesis that the rate of ripening is controlled at the genotypic level. Recent studies have explored the genetic determinants controlling the rate of ripening (Falginella *et al.*, 2025). As for the genotypes investigated in the present study, the horizontal separation between TSS curves of SR and NR (Figure 3A–C) indicates that the predominant explanatory variable is the shift in the onset of ripening. To understand the contribution of ripening rate to the SR trait, TSS and sugar content observations were modelled to extract ripening rates as TSS/day. In previous studies, sigmoid functions have been successfully used to characterise sugar accumulation in grapes, with good results when using TSS or sugar concentrations in g/L (de Rességuier *et al.*, 2024; Sadras *et al.*, 2008). Three-parameter sigmoid functions have been typically used to describe sugar changes over time (*i.e.*, DOY). These models set a fixed lower asymptote (*i.e.*, pre-veraison TSS values) and return three parameters, namely the upper asymptote, inflexion point and slope of the curve. In the present study, a five-parameter sigmoid curve that allows for a flexible lower asymptote and includes an asymmetry coefficient (Table 1) provided more satisfactory results for two reasons. First, it was observed that the lower asymptote varied both year-to-year and according to the genotype. Second, the asymmetry coefficient provided greater flexibility to capture differences in the transitions between the lower or upper asymptote and the inflexion point. The asymmetry was especially evident in the case of the SR genotype, where the three- and four-parameter fits did not converge or provided the worst fits across the three years (Figure S3). This was due to slow but steady increases from 5 to about 8.5 °Brix leading up to veraison (TSS curves for SR genotype in Figure 2A–C). TSS/day values extracted from five-parameter models were significantly higher in NR compared to SR across two years (Table 1 and Figure S3), suggesting ripening may be delayed and slower at the same time in the SR genotype. Similarly, different rates of ripening could be observed when aligning TSS curves based on the time of veraison (Figure S6). The lack of differences in TSS/day across genotypes in 2024 may be explained by the exceptionally hot and dry July (Figure 2, 15 days with Tmax $\geq$ 40 °C in 2024 compared to 6 and 0 days in 2023 and 2025, respectively), which corresponds with the time of ripening of NR fruit and likely provided supra-optimal conditions for sugar accumulation (Greer & Weston, 2010). When expressed as TSS/day, ripening rates cannot fully describe genotype-specific variation in sugar accumulation, as the latter is mixed with environmental factors (Duchêne *et al.*, 2012). This represented an important obstacle in our study, where it was found that sugar accumulation started and was completed by the end of July in NR, while SR started to ripen mid-September, under much cooler and shorter days. To account for these differences, ripening data were also modelled based on thermal time (GDD), and this approach was applied to TSS data (Table 1 and Figure S3) and sugar content estimates (Table S2 and Figure S4). GDD-based models allowed the removal of the interference of environmental conditions and focused on genotypic differences, removing the highly significant effects of the Year and Genotype *x* Year interaction factors observed in models by DOY (Table 1). Ripening rates were essentially unchanged in GDD-based models, signifying that the NR and SR genotypes display inherently equal sugar loading capabilities. Modelling estimates of sugar content per berry by DOY and GDD led to a similar result, with unchanged sugar loading rates (mg of sugar/berry) between NR and SR fruit (Table S2). Enhanced sugar loading rates were observed for Muscat of Alexandria, driven by large berries and possibly skewed by the methodology adopted to estimate sugar content. Our simplified estimation of sugar content per berry assumed constant sugar concentration across the entire berry weight, which does not account for seed weight and differences in sugar concentration by berry tissue (Possner & Kliewer, 1985; Ristic & Iland, 2005). Validation of sugar content results requires further work with measurements conducted on deseeded berries, given the strong genotypic determination of factors which could confound final sugar content estimates. Another result of interest that may be partly linked to environmental differences is the lower levels of final TSS measured in SR berries at the end of the season, well below 20 °Brix in all years (Table 1). A combination of less favourable temperatures for plant metabolism and senescence may play a role in the plateauing of sugar accumulation around 15 to 17 °Brix. Whether this is the maximum berry sugar accumulation in the SR genotype or ripening could continue in the presence of favourable conditions, it remains unsubstantiated, and it could be the object of future research in controlled conditions. The maximum sugar ripeness measured in SR fruit is likely to be suboptimal for winegrapes, except for low alcohol wines. The development of other fruit quality traits would also need to be screened to verify the oenological aptitude of this material.

2. First insights on slow ripening mechanisms

A series of targeted manipulatory experiments were conducted to gather initial insights regarding potential reasons behind the large lag and slower ripening described in detail above for SR. Three hypotheses were formulated as possible causes for this unique phenotypic variant. In screening different rescuing treatments, the metric of success was to capture a rapid initiation of ripening in treated SR fruit compared to the untreated control.

First, we tested the possibility of carbon constraint at the leaf level by analysing physiological processes in leaves of the NR and SR. Carbon limitation may occur because of damaged photosynthesis machinery or a structural blockage of vascular systems in charge of carbon translocation (*i.e.*, phloem). Physiological measurements at the leaf level, taken during the long lag phase of SR over two years, showed no limitation in terms of carbon assimilation (Figure 4). Similarly, no colour or textural symptoms associated with sugar build-up in leaves were observed in the field until senescence, such as leaf reddening and curling (data not shown). These symptoms are often reported for virus-infected vines due to the pathogenic agent blocking the sugar transportation mechanism (Song *et al.*, 2021; Sudarshana *et al.*, 2015).

The second hypothesis was that the ripening delay could be attributed to source–sink regulation, ultimately through improper balance between fruit weight (sink) and leaf area (source). This ratio, more often called crop load, has been widely studied in grapes and was shown to be tightly related to sugar maturity at harvest (Kliewer & Dokoozlian, 2005). Crop load was also found to be a main driver for ripening rate (Cameron *et al.*, 2021). Ripening is reported to be delayed in overcropping conditions, and cluster thinning can advance the onset of ripening (Petrie & Clingeleffer, 2006; Previtali *et al.*, 2021). Severe cluster removal applied at key stages did not advance the onset of ripening in SR (Figure 6). This result is in contrast with outcomes of this practice in the literature (reviewed in Vanderweide *et al.*, 2024) and provides experimental evidence that the slow ripening is not the result of crop load limitations.

Another plausible hypothesis was that there is a failure in the processes leading to the initiation of ripening. Lack of inactivation of one or more processes required for berries to start ripening may explain the extended lag phase observed for SR (Figure 3). Experimental treatments were applied to compensate for physiological events that were potentially latent in SR fruit (Castellarin *et al.*, 2016). The same dose of a surfactant compound (Tween20®) was applied in addition to each softening agent or plant growth regulator. When applied as a standalone, the Tween treatment was not significantly different from untreated fruit in terms of both the onset and rate of ripening, and there were only transient differences at later stages, likely due to vine and cluster variability (Figure 5 and 7C,F,I). The effect of adding a surfactant was absent in both the 2022 and 2023 experiments, excluding the possibility of artefacts when interpreting the effect of target compounds. Specific agents were used to induce softening (PEG), sugar accumulation (SUC) and signalling (ABA and ACC). Softening of grape berries is hypothesised to occur due to a shift from symplasmic to apoplasmic phloem unloading, causing a reduction in turgor and the start of rapid sugar accumulation (Zhang *et al.*, 2006). Failure to soften, as characterised by berry firmness measurements (Figure 3G–I), may be the limiting factor preventing rapid sugar accumulation and interfering with the transition of phloem unloading routes. PEG and SUC applications were aimed at inducing berry softening and subsequent sugar accumulation by increasing solute concentrations in the apoplast. PEG was selected as a softening agent that would remain confined in the apoplast given its inability to cross cell membranes, avoiding possible confounding effects of sucrose uptake into the cells. Both PEG and SUC treatments were ineffective (Figure 3), aside from transient significant differences that are explained by vine-to-vine variation since treatments were applied on adjacent vines. PEG caused an apparent increase in TSS; however, this was only true at the end of the season, and there was no sign of advanced ripening. These discrepancies are to be attributed to two main factors. First, PEG treatment was highly concentrated, and the compound itself resulted in TSS increases (100 g/L PEG solution = 9.0 °Brix). Even though berries were rinsed prior to TSS analysis, a fraction of the agent was expected to penetrate berries from the time of treatment, interfering with grape-derived sugars. As for the late season TSS effect, high concentrations of PEG spray led to crystallisation on berries, possibly causing more rapid dehydration and increased sugar concentration in the berries. The inefficacy of PEG and SUC may be explained by insufficient solute concentration reaching the apoplast, but based on the results observed for ABA treatments, it is more likely that the failure in ripening observed in the SR selection is related to disrupted hormone signalling.

The goal of treating SR fruit with ABA and ACC was to evaluate whether hormonal mechanisms beyond solute gradient dynamics impeded ripening in the SR genotype. Although grapes are non-climacteric fruit, there is evidence for ethylene biosynthesis and crosstalk with other phytohormones at the onset of grape ripening (Böttcher *et al.*, 2013; Chervin & Deluc, 2010; Chervin *et al.*, 2004). Extensive work on the involvement of ethylene in fruit ripening-related processes has been conducted using ethylene-releasing compounds (2-choroethylphosponic acid [CEPA]) or precursors of ethylene inhibitors (1-methylcyclopropane [1-MCP]). ACC is an intermediate for ethylene biosynthesis, and its application has been recently shown to positively influence colour development in table grapes, with negligible effects on sugar accumulation (de Aguiar *et al.*, 2024). Exogenous ACC applications conducted using the same commercial product as in de Aguiar *et al.* (2024) were not effective at advancing ripening of SR fruit in the present study (Figure 5A). These results add to existing work on ethylene in grapes and point to its far from fully understood involvement in berry ripening. Due to the lack of effects observed in our first trial, larger attention was given to the highly significant ABA treatments that resulted in the desired outcome of rescuing ripening. The role of ABA in grape ripening has been thoroughly investigated, and its involvement in triggering malate and sugar transport to the apoplast has been demonstrated (Castellarin *et al.*, 2011; Pilati *et al.*, 2017). ABA is also hypothesised to contribute to the regulation of grape berry ripening in other ways that are still not fully elucidated. Over three years, substantial evidence was collected on the efficacy of ABA to rescue ripening in the SR genotype (Figure 3 and Figure 7), which points to incomplete signalling being the most likely reason for the delayed sugar accumulation

of the SR genotype. The limited effect of the lower dosage (400 ppm) compared to the prompt response to the highest rate (2000 ppm), suggests suboptimal endogenous levels of ABA in the SR fruit. The timing effect observed in experiment 4 (Figure 7) further confirms that SR fruit had reached a state of proneness to ripen, which was only realised when appropriate levels of chemical signals were delivered to the berry via exogenous treatments. Similarly, we observed that seed maturity in the SR genotype is reached at the end of the green phase, excluding improper seed maturation from being the main factor (data not shown). The hypothesis of limitations in ABA-related pathways is further corroborated by the effect of drying down SR vines in experiment 5, where the WS treatment promptly triggered ripening at the same time as ABA2000 exogenous application (Figure 8). Notably, ABA2000 and WS applied to SR fruit caused TSS accumulation to start at the same time; however, with a more marked accumulation in ABA2000. It is possible that photosynthesis rates were reduced in WS vines concurrently with the measured drop in gs, as previously reported (Gambetta *et al.*, 2020). Such limitation to water and photosynthate allocation to the fruit is the likely cause behind the differences in berry weights between ABA2000 and WS fruit, affecting the final sugar content per berry (Figure S7). The pivotal role of ABA in the reorganisation of berry processes marking the transition from pre- to post-veraison stages is well established (Castellarin *et al.*, 2016; Pilati *et al.*, 2017). As to the SR genotype, a mechanistic explanation for impeded ripening remains unsubstantiated. Given the interplay between ABA and other hormones (Böttcher *et al.*, 2013; Böttcher *et al.*, 2010; Dal Santo *et al.*, 2020; Gouthu & Deluc, 2015), insufficient auxin sequestration and improper ABA biosynthesis or their interaction are all possible reasons. ABA catabolism may also be enhanced in the SR genotype, leading to lower levels of active ABA than those required to counterbalance auxins (Owen *et al.*, 2009). Since natural ABA was used in our trials, experimenting with ABA analogues with longer residual activity in plants and/or analysis of ABA catabolites would allow us to investigate the direct effect of ABA and its fate in SR fruit. To clarify the interactive role of ABA and auxins and the mode of action of exogenous ABA, hormone profiling represents a necessary next step for this research. Based on recent advancements in grape functional genomics, differential expression analysis of genes involved in ripening signalling or regulation would provide important insights into the mechanisms behind the SR trait described in this study. Alongside fundamental work, segregation studies are required to understand the genetic basis of the slow ripening trait and develop tools to incorporate it through traditional or new-generation breeding techniques.

CONCLUSION

Screening of material displaying phenotypic variation in the dynamics of sugar accumulation represents the basis for developing long-term strategies to cope with a warmer climate and advanced grape maturity. We characterised physiological aspects of ripening in fruit of a slow ripening genotype and found that ripening was delayed by more than 65 days over three years. The rate of sugar accumulation was slower, but to a lower degree. Although this delay may be excessive for commercial applications, this material offers a unique opportunity to explore mechanisms of slow ripening in grapevines. Preliminary experiments on carbon limitation at the leaf level and using severe crop removal to address potential unbalance in source-sink relationships suggested that impediments at these levels are unlikely. Conversely, sugar accumulation was triggered when exogenous ABA was applied to the fruit. These insights are the foundation for future studies on regulatory mechanisms, which could lead the way for modulating this trait for vines better adapted to current climatic conditions.

ACKNOWLEDGEMENTS

The authors would like to acknowledge the Viticulture Research team at E. & J. Gallo Winery for their precious support with the experimental trials: Nona Ebisuda for field work support; Don Katayama for help with chemical application; Cella Bioni, Miriam Villa and Jared Nicholson for help with sample collection and processing. We appreciate Lindon Inouye from Valent Biosciences for generously providing chemical products used in the trial.

AUTHOR CONTRIBUTIONS

PP, PC, MB, and ND conceptualised and designed the study; PP, EG and OB collected data in the field and performed data analysis; KS provided the Grape Grabber and assistance with data processing and interpretation; MF and SZ helped with data interpretation. All authors have contributed to data interpretation and manuscript writing and have read and approved this manuscript before its submission.

REFERENCES

Böttcher, C., Burbidge, C. A., Boss, P. K., & Davies, C. (2013). Interactions between ethylene and auxin are crucial to the control of grape (*Vitis vinifera* L.) berry ripening. *BMC Plant Biology*, *13*(1). https://doi.org/10.1186/1471-2229-13-222

Böttcher, C., Harvey, K. E., Forde, C. G., Boss, P. K., & Davies, C. (2011). Auxin treatment of pre-veraison grape (*Vitis vinifera* L.) berries both delays ripening and increases the synchronicity of sugar accumulation. *Australian Journal of Grape and Wine Research*, *17*(1), 1–8. https://doi.org/10.1111/j.1755-0238.2010.00110.x

Böttcher, C., Keyzers, R. A., Boss, P. K., & Davies, C. (2010). Sequestration of auxin by the indole-3-acetic acid-amido synthetase GH3-1 in grape berry (*Vitis vinifera* L.) and the proposed role of auxin conjugation during ripening. *Journal of Experimental Botany*, *61*(13), 3615–3625. https://doi.org/10.1093/jxb/erq174

Cameron, W., Petrie, P. R., Barlow, E. W. R., Patrick, C. J., Howell, K., & Fuentes, S. (2021). Is advancement of grapevine maturity explained by an increase in the rate of ripening or advancement of veraison? *Australian Journal of Grape and Wine Research*, *27*(3), 1–14. https://doi.org/10.1111/ajgw.12481

Castellarin, S. D., Gambetta, G. A., Wada, H., Krasnow, M. N., Cramer, G. R., Peterlunger, E., Shackel, K. A., & Matthews, M. (2016). Characterization of major ripening events during softening in grape: Turgor, sugar accumulation, abscisic acid metabolism, colour development, and their relationship with growth. *Journal of Experimental Botany*, *67*(3), 709–722. https://doi.org/10.1093/jxb/erv483

Castellarin, S. D., Gambetta, G. A., Wada, H., Shackel, K. A., & Matthews, M. A. (2011). Fruit ripening in *Vitis vinifera*: Spatiotemporal relationships among turgor, sugar accumulation, and anthocyanin biosynthesis. *Journal of Experimental Botany*, *62*(12), 4345–4354. https://doi.org/10.1093/jxb/err150

Chervin, C., & Deluc, L. (2010). Ethylene signalling receptors and transcription factors over the grape berry development: gene expression profiling. *Vitis*, *3*, 129–136. https://doi.org/10.5073/vitis.2010.49.129-136

Chervin, C., El-Kereamy, A., Roustan, J. P., Latché, A., Lamon, J., & Bouzayen, M. (2004). Ethylene seems required for the berry development and ripening in grape, a non-climacteric fruit. *Plant Science*, *167*(6), 1301–1305. https://doi.org/10.1016/J.PLANTSCI.2004.06.026

Coombe, B. G. (1992). Research on development and ripening of the grape berry. *American Journal of Enology and Viticulture*, *43*(1), 101–110. https://doi.org/10.5344/ajev.1992.43.1.101

Dal Santo, S., Tucker, M. R., Tan, H. T., Burbidge, C. A., Fasoli, M., Böttcher, C., Boss, P. K., Pezzotti, M., & Davies, C. (2020). Auxin treatment of grapevine (*Vitis vinifera* L.) berries delays ripening onset by inhibiting cell expansion. *Plant Molecular Biology*, *103*(1–2), 91–111. https://doi.org/10.1007/s11103-020-00977-1

de Aguiar, A. C., Yamashita, F., Koyama, R., Caetano, B. E. B., Utiamada, C. A. K., & Roberto, S. R. (2024). Exogenous application of 1-aminocyclopropane-1-carboxylic acid as a new strategy to trigger the color development of table grapes grown in subtropics. *Horticulturae*, *10*(12), 1276. https://doi.org/10.3390/HORTICULTURAE10121276/S1

de Rességuier, L., Inchboard, L., Parker, A.K., Petitjean, T., van Leeuwen, C. (2024). Drivers of grape berry sugar accumulation in field conditions at local scale. *OENO One 58*(4). https://doi.org/10.20870/oeno-one.2024.58.4.8195

Deloire, A. (2011). The concept of berry sugar loading. *Wineland Magazine*, 81–83.

Duchêne, E., Dumas, V., Jaegli, N., & Merdinoglu, D. (2012). Deciphering the ability of different grapevine genotypes to accumulate sugar in berries. *Australian Journal of Grape and Wine Research*, *18*(3), 319–328. https://doi.org/10.1111/j.1755-0238.2012.00194.x

Falginella, L., Magris, G., Castellarin, S. D., Gambetta, G. A., Matthews, M. A., Morgante, M., & Di Gaspero, G. (2025). Grape ripening speed slowed down using natural variation. *Theoretical and Applied Genetics, 138(6)*, 130. https://doi.org/ 10.1007/s00122-025-04914-y

Faralli, M., Mallucci, S., Bignardi, A., Varner, M., & Bertamini, M. (2024). Four decades in the vineyard: the impact of climate change on grapevine phenology and wine quality in northern Italy. *OENO One*, *58*(3). https://doi.org/10.20870/OENO-ONE.2024.58.3.8083

Fasoli, M., Richter, C. L., Zenoni, S., Bertini, E., Vitulo, N., Dal Santo, S., Dokoozlian, N., Pezzotti, M., & Tornielli, G. B. (2018). Timing and order of the molecular events marking the onset of berry ripening in grapevine. *Plant Physiology*, *178*, 1187–1206. https://doi.org/10.1104/pp.18.00559

Fraga, H., García de Cortázar Atauri, I., Malheiro, A. C., & Santos, J. A. (2016). Modelling climate change impacts on viticultural yield, phenology and stress conditions in Europe. *Global Change Biology*, *22*(11), 3774–3788. https://doi.org/10.1111/gcb.13382

Fraga, H., Malheiro, A. C., Moutinho-Pereira, J., & Santos, J. A. (2012). An overview of climate change impacts on European viticulture. *Food and Energy Security*, *1*(2), 94–110. https://doi.org/10.1002/fes3.14

Frioni, T., Romanini, E., Pagani, S., Del Zozzo, F., Lambri, M., Vercesi, A., Gatti, M., Poni, S., & Gabrielli, M. (2023). Reintroducing autochthonous minor grapevine varieties to improve wine quality and viticulture sustainability in a climate change scenario. *Australian Journal of Grape and Wine Research*, *2023*. https://doi.org/10.1155/2023/1482548

Frioni, T., Squeri, C., Del Zozzo, F., Guadagna, P., Gatti, M., Vercesi, A., & Poni, S. (2021). Investigating evolution and balance of grape sugars and organic acids in some new pathogen-resistant white grapevine varieties. *Horticulturae*, *7*(8). https://doi.org/10.3390/horticulturae7080229

Gambetta, G.A., Herrera, J.C., Dayer, S., Feng, Q., Hochberg, U., & Castellarin, S.D. (2020). The physiology of drought stress in grapevine: towards an integrative definition of drought tolerance. *J Exp Bot* 71:4658–4676. https://doi.org/10.1093/jxb/eraa245

Gouthu, S., & Deluc, L. G. (2015). Timing of ripening initiation in grape berries and its relationship to seed content and pericarp auxin levels. *BMC Plant Biology*, *15*(1), 46. https://doi.org/10.1186/s12870-015-0440-6

Greer, D.H., & Weston, C. (2010). Heat stress affects flowering, berry growth, sugar accumulation and photosynthesis of Vitis vinifera cv. Semillon grapevines grown in a controlled environment. *Functional Plant Biology* 37:206–214. https://doi.org/10.1071/FP09209

Gutiérrez-Gamboa, G., Zheng, W., & Martínez de Toda, F. (2021). Current viticultural techniques to mitigate the effects of global warming on grape and wine quality: A comprehensive review. *Food Research International*, *139*. https://doi.org/10.1016/j.foodres.2020.109946

Jarvis, C., Darbyshire, R., Goodwin, I., Barlow, E. W. R., & Eckard, R. (2019). Advancement of winegrape maturity continuing for winegrowing regions in Australia with variable evidence of compression of the harvest period. *Australian Journal of Grape and Wine Research*, *25*(1), 101–108. https://doi.org/10.1111/ajgw.12373

Jones, G. V. (2010). Climate, grapes and wine: Structure and sustainability in a variable and changing climate. *VIII International Terroir Congress*.

Jones, G. V., & Davis, R. E. (2000). Climate influences on grapevine phenology, grape composition, and wine production and quality for Bordeaux, France. *American Journal of Enology and Viticulture*, *51*(3), 249–261. https://doi.org/10.5344/ajev.2000.51.3.249

Jones, G. V., & Webb, L. B. (2010). Climate Change, Viticulture, and Wine: Challenges and Opportunities. *Journal of Wine Research*, *21*(2–3), 103–106. https://doi.org/10.1080/09571264.2010.530091

Kliewer, W. M., & Dokoozlian, N. K. (2005). Leaf area/crop weight ratios of grapevines: Influence on fruit composition and wine quality. *American Journal of Enology and Viticulture*, *56*(2), 170–181. https://doi.org/10.5344/ajev.2005.56.2.170

Kuznetsova, A., Brockhoff, P. B., & Christensen, R. H. B. (2017). lmerTest package: Tests in linear mixed effects models. *Journal of Statistical Software*, *82*(13), 1–26. https://doi.org/10.18637/jss.v082.i13

Lenth, R. (2020). *emmeans: Estimated marginal means, aka least-squares means*. (R package version 1.4.5). https://cran.r-project.org/package=emmeans

Mira de Orduña, R. (2010). Climate change associated effects on grape and wine quality and production. *Food Research International*, *43*(7), 1844–1855. https://doi.org/10.1016/j.foodres.2010.05.001

Mori, K., Goto-Yamamoto, N., Kitayama, M., & Hashizume, K. (2007). Loss of anthocyanins in red-wine grape under high temperature. *Journal of Experimental Botany*, *58*(8), 1935–1945. https://doi.org/10.1093/jxb/erm055

Novello, V., & de Palma, L. (2013). Viticultural strategies to reduce alcohol levels in wine. *Alcohol Level Reduction in Wine - Oenoviti International Network*.

Owen, S. J., Lafond, M. D., Bowen, P., Bogdanoff, C., Usher, K., & Abrams, S. R. (2009). Profiles of abscisic acid and its catabolites in developing Merlot grape (*Vitis vinifera*) berries. *American Journal of Enology and Viticulture*, *60*(3), 277–284. https://doi.org/10.5344/AJEV.2009.60.3.277

Palliotti, A., Tombesi, S., Silvestroni, O., Lanari, V., Gatti, M., & Poni, S. (2014). Changes in vineyard establishment and canopy management urged by earlier climate-related grape ripening: A review. *Scientia Horticulturae*, *178*, 43–54. https://doi.org/10.1016/j.scienta.2014.07.039

Petrie, P. R., & Clingeleffer, P. R. (2006). Crop thinning (hand versus mechanical), grape maturity and anthocyanin concentration: Outcomes from irrigated Cabernet Sauvignon (*Vitis vinifera* L.) in a warm climate. *Australian Journal of Grape and Wine Research*, *12*(1), 21–29. https://doi.org/10.1111/j.1755-0238.2006.tb00040.x

Pilati, S., Bagagli, G., Sonego, P., Moretto, M., Brazzale, D., Castorina, G., Simoni, L., Tonelli, C., Guella, G., Engelen, K., Galbiati, M., & Moser, C. (2017). Abscisic acid is a major regulator of grape berry ripening onset: new insights into ABA signaling network. *Frontiers in Plant Science*, *8*, 1–16. https://doi.org/10.3389/fpls.2017.01093

Poni, S., Sabbatini, P., & Palliotti, A. (2022). Facing spring frost damage in grapevine: Recent developments and the role of delayed winter pruning – A review. *American Journal of Enology and Viticulture*, *73*(4), 211–226. https://doi.org/10.5344/AJEV.2022.22011

Possner, D., & Kliewer, W. (1985). The localisation of acids, sugars, potassium and calcium in developing grape berries. *Vitis, 24*(4), 229-240. https://doi.org/10.5073/vitis.1985.24.229-240

Previtali, P., Dokoozlian, N. K., Pan, B. S., Wilkinson, K. L., & Ford, C. M. (2021). Crop load and plant water status influence the ripening rate and aroma development in berries of grapevine (*Vitis vinifera* L.) cv. Cabernet Sauvignon. *Journal of Agricultural and Food Chemistry*, *69*(27), 7709–7724. https://doi.org/10.1021/acs.jafc.1c01229

Previtali, P., Giorgini, F., Mullen, R. S., Dokoozlian, N. K., Wilkinson, K. L., & Ford, C. M. (2022). A systematic review and meta-analysis of vineyard techniques used to delay ripening. *Horticulture Research*. https://doi.org/10.1093/hr/uhac118

R Core Team. (2012). *R: A language and environment for statistical computing*.

Rienth, M., Torregrosa, L., Sarah, G., Ardisson, M., Brillouet, J. M., & Romieu, C. (2016). Temperature desynchronizes sugar and organic acid metabolism in ripening grapevine fruits and remodels their transcriptome. *BMC Plant Biology*, *16*, 164. https://doi.org/10.1186/s12870-016-0850-0

Ristic, R., & Iland, P.G. (2005). Relationships between seed and berry development of *Vitis Vinifera* L. cv Shiraz: Developmental changes in seed morphology and phenolic composition. *Australian Journal of Grape and Wine Research*, *11*:43–58. https://doi.org/10.1111/j.1755-0238.2005.tb00278.x

Ritz, C., Baty, F., Streibig, J. C., & Gerhard, D. (2015). Dose-response analysis using R. *PLoS ONE*, *10*(12). https://doi.org/10.1371/journal.pone.0146021

Rogiers, S. Y., Greer, D. H., Liu, Y., Baby, T., & Xiao, Z. (2022). Impact of climate change on grape berry ripening: An assessment of adaptation strategies for the Australian vineyard. *Frontiers in Plant Science*, *13*, 1094633. https://doi.org/10.3389/FPLS.2022.1094633/PDF

Sadras, V.O., Collins, M., Soar, C.J. (2008). Modelling variety-dependent dynamics of soluble solids and water in berries of *Vitis vinifera*. *Aust J Grape Wine Res* 14:250–259. https://doi.org/10.1111/j.1755-0238.2008.00025.x

Sadras, V., & Moran, M. A. (2012). Elevated temperature decouples anthocyanins and sugars in berries of Shiraz and Cabernet Franc. *Australian Journal of Grape and Wine Research*, *18*(2), 115–122. https://doi.org/10.1111/j.1755-0238.2012.00180.x

Sadras, V., & Petrie, P. R. (2011). Quantifying the onset, rate and duration of sugar accumulation in berries from commercial vineyards in contrasting climates of Australia. *Australian Journal of Grape and Wine Research*, *17*(2), 190–198. https://doi.org/10.1111/j.1755-0238.2011.00135.x

Sadras, V., Petrie, P. R., & Moran, M. A. (2013). Effects of elevated temperature in grapevine. II juice pH, titratable acidity and wine sensory attributes. *Australian Journal of Grape and Wine Research*, *19*(1), 107–115. https://doi.org/10.1111/ajgw.12001

Shahood, R., Torregrosa, L., Savoi, S., & Romieu, C. (2020). First quantitative assessment of growth, sugar accumulation and malate breakdown in a single ripening berry. *OENO One*, *4*, 1077–1092. https://doi.org/10.20870/oeno-one.2020.54.4.3787

Song, Y., Hanner, R. H., & Meng, B. (2021). Probing into the Effects of Grapevine Leafroll-Associated Viruses on the Physiology, Fruit Quality and Gene Expression of Grapes. *Viruses*, *13*(4), 593. https://doi.org/10.3390/V13040593

Stanfield, R. C., Forrestel, E. J., Elmendorf, K. E., Bagshaw, S. B., & Bartlett, M. K. (2024). Phloem anatomy predicts berry sugar accumulation across 13 wine-grape cultivars. *Frontiers in Plant Science*, *15*, 1360381. https://doi.org/10.3389/FPLS.2024.1360381/BIBTEX

Sudarshana, M. R., Perry, K. L., & Fuchs, M. F. (2015). Grapevine red blotch-associated virus, an emerging threat to the grapevine industry. *Phytopathology*, *105*(7), 1026–1032. https://doi.org/10.1094/PHYTO-12-14-0369-FI

Sweetman, C., Sadras, V., Hancock, R. D., Soole, K. L., & Ford, C. M. (2014). Metabolic effects of elevated temperature on organic acid degradation in ripening *Vitis vinifera* fruit. *Journal of Experimental Botany*, *65*(20), 5975–5988. https://doi.org/10.1093/jxb/eru343

Tavernier, F., Savoi, S., Torregrosa, L., Hugueney, P., Baltenweck, R., Segura, V., & Romieu, C. (2025). The single-berry metabolomic clock paradigm reveals new stages and metabolic switches during grapevine berry development. *Journal of Experimental Botany*. https://doi.org/10.1093/JXB/ERAF038

Tilbrook, J., & Tyerman, S. D. (2008). Cell death in grape berries: Varietal differences linked to xylem pressure and berry weight loss. *Functional Plant Biology*, *35*(3), 173–184. https://doi.org/10.1071/FP07278

U.S. Geological Survey. (2024). *U.S. Geological Survey*.

van Leeuwen, C., & Darriet, P. (2016). The impact of climate change on viticulture and wine quality. *Journal of Wine Economics*, *11*(1), 150–167. https://doi.org/10.1017/jwe.2015.21

van Leeuwen, C., Sgubin, G., Bois, B., Ollat, N., Swingedouw, D., Zito, S., & Gambetta, G. A. (2024). Climate change impacts and adaptations of wine production. In *Nature Reviews Earth and Environment* (Vol. 5, Issue 4, pp. 258–275). Springer Nature. https://doi.org/10.1038/s43017-024-00521-5

Vanderweide, J., Nasrollahiazar, E., Schultze, S., Sabbatini, P., & Castellarin, S. D. (2024). Impact of cluster thinning on wine grape yield and fruit composition: A review and meta-analysis. *Australian Journal of Grape and Wine Research*, *2024*(1), 2504396. https://doi.org/10.1155/2024/2504396

Wada, H., Matthews, M. A., & Shackel, K. A. (2009). Seasonal pattern of apoplastic solute accumulation and loss of cell turgor during ripening of *Vitis vinifera* fruit under field conditions. *Journal of Experimental Botany*, *60*(6), 1773–1781. https://doi.org/10.1093/jxb/erp050

Webb, L. B., Whetton, P. H., & Barlow, E. W. R. (2007). Modelled impact of future climate change on the phenology of winegrapes in Australia. *Australian Journal of Grape and Wine Research*, *13*(3), 165–175. https://doi.org/10.1111/j.1755-0238.2007.tb00247.x

Webb, L. B., Whetton, P. H., & Barlow, E. W. R. (2011). Observed trends in winegrape maturity in Australia. *Global Change Biology*, *17*(8), 2707–2719. https://doi.org/10.1111/J.1365-2486.2011.02434.X

Webb, L. B., Whetton, P. H., Bhend, J., Darbyshire, R., Briggs, P. R., & Barlow, E. W. R. (2012). Earlier wine-grape ripening driven by climatic warming and drying and management practices. *Nature Climate Change 2012 2:4*, *2*(4), 259–264. https://doi.org/10.1038/nclimate1417

Wickham, H. (2016). *ggplot2: Elegant graphics for data analysis* (R. Gentleman, K. Hornik, & G. Parmigiani, Eds.; 2nd ed.). Springer International Publishing.

Zenoni, S., Ferrarini, A., Giacomelli, E., Xumerle, L., Fasoli, M., Malerba, G., Bellin, D., Pezzotti, M., & Delledonne, M. (2010). Characterization of transcriptional complexity during berry development in *Vitis vinifera* using RNA-Seq. *Plant Physiology*, *152*(4), 1787–1795. https://doi.org/10.1104/pp.109.149716

Zhang, X. Y., Wang, X. L., Wang, X. F., Xia, G. H., Pan, Q. H., Fan, R. C., Wu, F. Q., Yu, X. C., & Zhang, D. P. (2006). A shift of phloem unloading from symplasmic to apoplasmic pathway is involved in developmental onset of ripening in grape berry. *Plant Physiology*, *142*(1), 220. https://doi.org/10.1104/PP.106.081430